Geochemical analysis of Atlantic Rim water, Carbon County, Wyoming: New applications for characterizing coalbed natural gas reservoirs

J. Fred McLaughlin, Carol D. Frost, and Shikha Sharma

ABSTRACT

Coalbed natural gas (CBNG) production typically requires the extraction of large volumes of water from target formations, thereby influencing any associated reservoir systems. We describe isotopic tracers that provide immediate data on the presence or absence of biogenic natural gas and the identify methane-containing reservoirs are hydrologically confined. Isotopes of dissolved inorganic carbon and strontium, along with water quality data, were used to characterize the CBNG reservoirs and hydrogeologic systems of Wyoming's Atlantic Rim. Water was analyzed from a stream, springs, and CBNG wells.

Strontium isotopic composition and major ion geochemistry identify two groups of surface water samples. Muddy Creek and Mesaverde Group spring samples are Ca-Mg-SO_4–type water with higher $^{87}Sr/^{86}Sr$, reflecting relatively young groundwater recharged from precipitation in the Sierra Madre. Groundwaters emitted from the Lewis Shale springs are Na-HCO_3–type waters with lower $^{87}Sr/^{86}Sr$, reflecting sulfate reduction and more extensive water-rock interaction.

To distinguish coalbed waters, methanogenically enriched $\delta^{13}C_{DIC}$ was used from other natural waters. Enriched $\delta^{13}C_{DIC}$, between –3.6 and +13.3‰, identified spring water that likely originates from Mesaverde coalbed reservoirs. Strongly positive $\delta^{13}C_{DIC}$, between +12.6 and +22.8‰, identified those coalbed reservoirs that are confined, whereas lower $\delta^{13}C_{DIC}$, between +0.0 and +9.9‰, identified wells within unconfined reservoir systems.

Manuscript received November 24, 2009; provisional acceptance February 11, 2010; revised manuscript received May 17, 2010; final acceptance June 30, 2010.
DOI:10.1306/06301009190

AUTHORS

J. Fred McLaughlin ~ *Wyoming State Geological Survey, Laramie, Wyoming; derf1@uwyo.edu*

Fred McLaughlin graduated with an M.S. degree in geology and geophysics from the University of Wyoming. He is the manager of the Regional Geology, Hydrology, and Mineral Resources Group at the Wyoming State Geological Survey. His research interests include investigating the interaction between hydrologic and hydrocarbon systems using isotopic geochemical studies and Laramide-related structural deformation.

Carol D. Frost ~ *Department of Geology and Geophysics, University of Wyoming, Laramie, Wyoming; frost@uwyo.edu*

Carol Frost graduated with a Ph.D. in Earth sciences from the University of Cambridge. She is a professor of geology and associate vice president for Research and Economic Development. Her research interests involve the application of isotopic tracers to varied problems from the origin and evolution of the continental crust to the geochemistry of water coproduced with coalbed natural gas.

Shikha Sharma ~ *Department of Geology and Geography, West Virginia University, Morgantown, West Virginia; shikha.sharma@mail.wvu.edu*

Shikha Sharma graduated with a Ph.D. in geology from the Center of Advanced Studies in Geology from the University of Lucknow. Shikha Sharma is an Assistant Professor of geology at West Virginia University. Her research interests are focused on applications of stable isotopes as natural tracers of different geochemical, biological, and climatic processes impacting our environment.

ACKNOWLEDGEMENTS

Funding for this study came through the Wyoming State Geological Survey and the Rawlins Bureau of Land Management (BLM) field office. We thank Andy Stone of the BLM for initiating this study; Anadarko Petroleum Corporation for their cooperation and collaboration; and former State Geologist Ron Surdam and colleagues at the Wyoming State Geological Survey for their support. We also thank the reviewers for their helpful comments. The AAPG Editor thanks the following reviewers for their work on this paper: Jack C. Pashin and the two anonymous reviewers.

These results demonstrate that $\delta^{13}C_{DIC}$ analysis provides immediate data to help identify Atlantic Rim groundwater sources, hydraulic reservoir confinement, springs associated with methanogenic coalbed reservoirs, areas of peak methanogenic activity, and to help assess gas potential and promote efficient CBNG production.

INTRODUCTION

Within a single gas field the amount of coalbed natural gas (CBNG) produced varies from well to well, and some wells may produce only water (Surdam et al., 2007; WOGCC, 2010). This variability can be the result of available gas in place but commonly is related to the heterogeneous geologic and hydrologic nature of CBNG reservoirs (Surdam et al., 2007). An analytical method that provides immediate cost-effective characterization of a CBNG reservoir would help optimize gas production.

In 2007, when the Bureau of Land Management ([BLM] 2007) issued a record of decision approving a proposed natural gas development project, the Atlantic Rim area of southwest Carbon County became the site for Wyoming's most recent commercial-scale CBNG development (BLM, 2007; WOGCC, 2010). This study focuses on using new applications of carbon isotopes, along with multivariate water analysis, to characterize the CBNG reservoirs and related hydrogeologic systems of the Atlantic Rim. This work is also intended to serve as a baseline study of the hydrologic systems in the Atlantic Rim, against which the effects of CBNG development might be assessed. This study is a cooperative effort between the Wyoming State Geological Survey, the University of Wyoming, and the Rawlins Bureau of Land Management (BLM) field office.

STRUCTURAL SETTING AND GENERAL GEOLOGIC BACKGROUND

The Atlantic Rim is a topographically high region of uplifted westerly dipping Cretaceous sedimentary rocks in south-central Wyoming that represents the border between the Sierra Madre and the Greater Green River Basin (Figure 1). The eolian Sand Hills border the Atlantic Rim's western boundary, and springs from the Sand Hills were sampled for this study (Figure 1). The Cretaceous formations targeted for this study are, from oldest to youngest, the Steele Shale, Mesaverde Group, and Lewis Shale (Figure 1). All were deposited during transgressive or regressive cycles of the great Cretaceous Western Interior seaway (Roehler, 1992).

Steele Shale

The Steele Shale, approximately 4500 ft (1371 m) thick, was deposited during an episode of marine regression (Roehler, 1992; Steidtmann, 1993). The Steele Shale is a thick sequence of fine-grained marine clay and shale, with some siltstone and sandstone.

Mesaverde Group

The Mesaverde Group includes four distinct formations that consist of sandstone, shale, siltstone, mudstone, and coal. The four formations of the Mesaverde Group in the Atlantic Rim area are, from oldest to youngest, the Haystack Mountains Formation, Allen Ridge Formation, Pine Ridge Sandstone, and the Almond Formation (Figure 1). The Allen Ridge, Pine Ridge, and Almond formations are targeted for Atlantic Rim CBNG production (WOGCC, 2010).

Water coproduced with CBNG is injected into the sandstone of the approximately 750- to 950-ft (228–290 m)-thick Haystack Mountains Formation (BLM, 2007). The Haystack Mountains Formation was chosen for water disposal because it contains approximately 485 ft (148 m) of sandstone with adequate injectivity. Thick, continuous, overlying shale beds in the Haystack Mountains and Allen Ridge formations act as confining layers for injected water.

Overlying the Haystack Mountains Formation, the Allen Ridge Formation is composed primarily of interbedded shale, sandstone, siltstone,

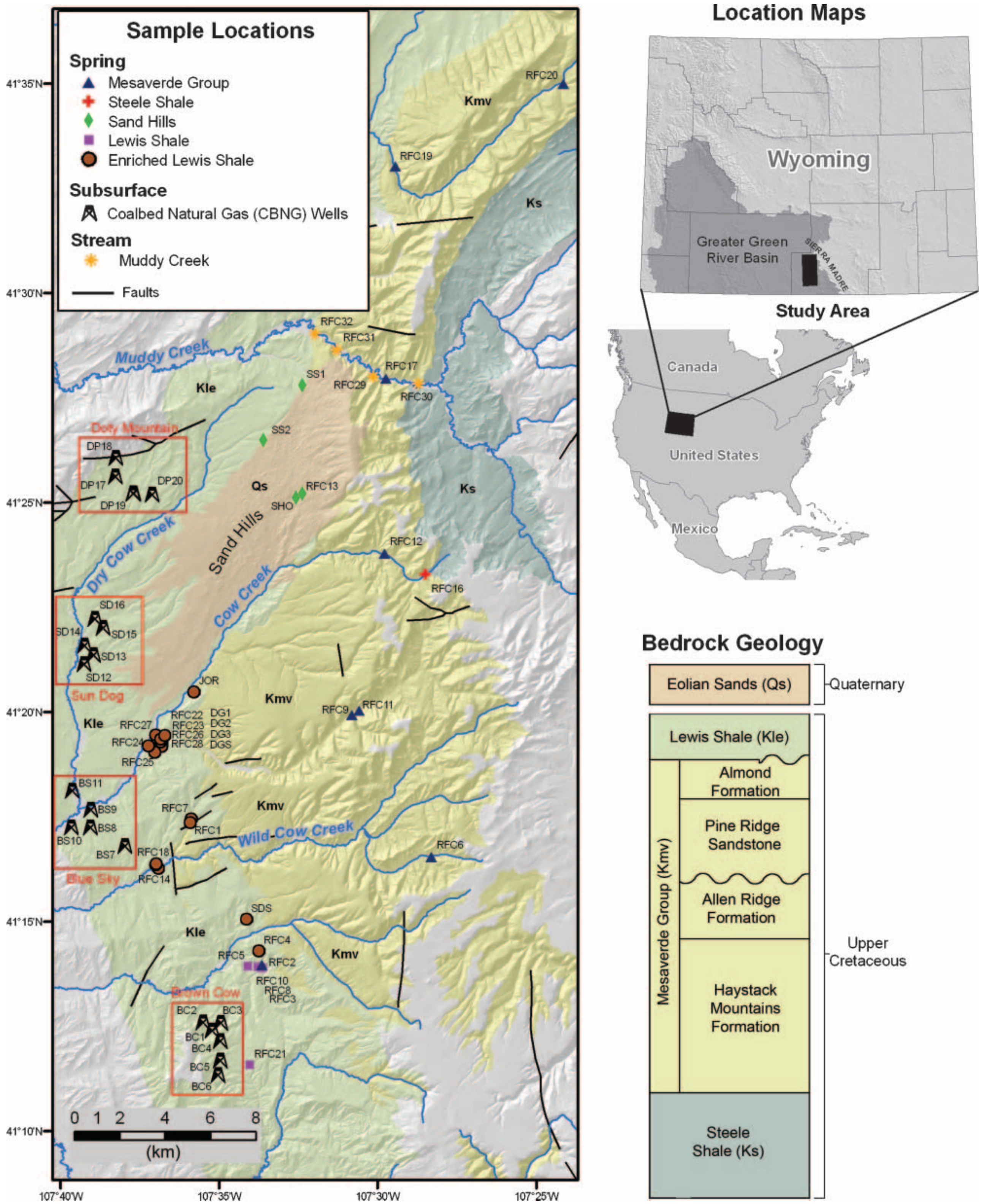

Figure 1. Atlantic Rim geologic map and stratigraphic column showing formations of interest and locations of sampled springs and CBNG wells (modified from Love and Christiansen, 1985).

and coal. Coal beds within the Allen Ridge Formation tend to thicken upward. The formation is 1200 to 1400 ft (366–427 m) thick in the Atlantic Rim area (Roehler, 1990; Hettinger et al., 2008).

The Pine Ridge Sandstone disconformably overlies the Allen Ridge Formation and is the only member of the Mesaverde Group that does not include marine deposits (Roehler, 1990; Hettinger et al., 2008). The Pine Ridge Sandstone, 40 to 100 ft (12–30 m) thick, consists mostly of cross-bedded sandstone, along with carbonaceous siltstone and thin localized coal beds (Roehler, 1990; Hettinger et al., 2008).

The Almond Formation, 450 to 550 ft (137–168 m) thick, overlies the Pine Ridge Sandstone and was deposited during westward marine transgression (Roehler, 1990; Hettinger et al., 2008). The Almond Formation consists of sandstone, shale, mudstone, claystone, and coal. The Almond Formation generally hosts the thickest coal beds in the Atlantic Rim area (Roehler, 1990; Hettinger et al., 2008).

Lewis Shale

The Lewis Shale overlies the Mesaverde Group and records the last marine sedimentation event of the Cretaceous. The Lewis Shale is composed of marine shale with interbedded sandstone and siltstone. The formation has a variable thickness across the study area but is approximately 2000 ft (610 m) thick. The basal unit is primarily shale with a low capacity for migrating fluids and acts as a confining layer to underlying Mesaverde Group reservoirs (Roehler, 1990; Hettinger and Roberts, 2005; Bartos et al., 2006). In the Atlantic Rim area, the Lewis Shale is thermally immature (measured vitrinite reflectance [R_o] values are <0.6) (Hettinger and Roberts, 2005).

Sand Hills

The southwest-to-northeast–trending Sand Hills are an extensive unconsolidated Quaternary eolian deposit that unconformably overlies Lewis Shale and abuts onto the westernmost outcrops of the Mesaverde Group in the north-central part of the study area (Figure 1) (Hettinger et al., 2008). The Sand Hills are approximately 10 mi long and up to 3 mi wide (16 × 4.8 km) (Figure 1).

ATLANTIC RIM COAL AND COALBED NATURAL GAS

Coalbed Natural Gas Systems and Coal of the Mesaverde Group

The Atlantic Rim CBNG system is currently modeled as a recharge-related stratigraphic trap (Lamarre and Ruhl, 2004; Johnson et al., 2005). Thermogenic gas is generated in deep sediments in the center of the Greater Green River Basin and migrates upward to the basin margins. The gas is adsorbed on Mesaverde Group coals by local hydraulic pressures which are regulated by recharge from the Sierra Madre (Roehler, 1990; Lamarre and Ruhl, 2004; Johnson et al., 2005). Recent work has shown a biogenic component in the CBNG of the Mesaverde Group (McLaughlin, 2009).

Mesaverde Group coals across the eastern Greater Green River Basin have undergone various degrees of thermal maturation (measured R_o values between <0.6 and 2.2) and are an established source of thermogenic natural gas in deeper areas of the basin (Roehler, 1990; Johnson et al., 2005). Mesaverde Group coals along the Atlantic Rim fall within the lowest ranks and are mostly high-volatile subbituminous C, with R_o values that are less than 0.6 (Roehler, 1990; Johnson et al., 2005). Most Mesaverde Group coals are less than 15 ft (4.5 m) thick, and CBNG production along the Atlantic Rim has focused on areas where the coals are stacked to maximize the amount of available pay (WOGCC, 2010). Preliminary adsorption isotherms generated with data from exploratory CBNG wells indicate that some coals were fully saturated with respect to gas (Lamarre and Ruhl, 2004).

Coalbed Natural Gas Development in the Atlantic Rim

The development of CBNG along the Atlantic Rim is projected to occur during a span of 20 yr,

Table 1. Water Chemistry and Isotopic Analysis Data for CBNG-Produced Water Samples*

Sample Number	TDS**	Ca^{2+}	Mg^{2+}	Na^{+}	K^{+}	Cl^{-}	SO_4^{2-}	HCO_3^{-}	CO_3^{2-}	F^{-}	Isotopic Analysis		Completion Date	Completions (depths from surface in ft)
											$^{87}Sr/^{86}Sr$	$\delta^{13}C_{DIC}$ (‰)		
Brown Cow Pod														
BC1	1693	2.0	<1	510.0	6.0	12.0	<1	1080.0	83.0	11.6	0.71028	1.1	2004	896–1120/1304–1423
BC2	2360	4.0	2.0	754.0	12.0	31.0	<1	1460.0	97.0	8.6	0.71100	3.9	2004	945–1165
BC3	1527	3.0	<1	461.0	6.0	6.0	<1	983.0	68.0	10.8	0.71055	0.6	2004	921–1143/1437–1446
BC4	1665	2.0	<1	500.0	6.0	5.0	<1	1070.0	82.0	13.5	0.71065	1.1	2004	1089–1285/1370–1568
BC5	2045	3.0	1.0	634.0	8.0	8.0	<1	1300.0	91.0	14.7	0.71103	5.1	2003	1010–1214/1429–1494
BC6	1719	3.0	<1	522.0	7.0	6.0	<1	1100.0	81.0	13.5	0.71059	1.3	2006	1029–1268
Averages	1835	2.8	1.0	563.5	7.5	11.3	<1	1165.5	83.7	12.1	0.71068	2.2		
Blue Sky Pod														
BS7	4097	15.0	7.0	1180.0	18.0	284.0	<1	2540.0	53.0	3.2	0.70944	14.3	2005	1012–1075/1266–1356
BS8	2757	12.0	5.0	761.0	15.0	234.0	<1	1730.0	<1	3.4	0.71040	12.6	2005	1914–2106/2292–2353
BS9	1557	2.0	<1	424.0	4.0	25.0	<1	1040.0	62.0	2.6	0.71028	0.0	2005	1441–1571/1711–1917/2053–2261
BS10	4250	21.0	8.0	1220.0	36.0	634.0	<1	2310.0	21.0	4.0	0.71208	18.8	2005	2311–2446/2676–2677
BS11	2464	7.0	3.0	722.0	18.0	71.0	<1	1580.0	63.0	6.6	0.70983	9.9	2005	1764–1834/1968–2091/2361–2404
Averages	3025	11.4	5.8	861.4	18.2	249.6	<1	1840.0	49.8	4.0	0.71041	11.1		
Sun Dog Pod														
SD12	3619	17.0	9.0	1030.0	28.0	279.0	<1	2190.0	66.0	5.8	0.71041	21.1	2005	953–1075/1242–1316
SD13	3364	13.0	6.0	950.0	20.0	244.0	<1	2050.0	81.0	4.8	0.71032	20.6	2005	833–965/1223–1390
SD14	3872	19.0	4.0	1060.0	20.0	240.0	<1	2430.0	99.0	4.2	0.71109	22.8	2005	868–969/1239–1302
SD15	4172	7.0	4.0	1200.0	21.0	268.0	<1	2530.0	142.0	5.7	0.71116	19.1	2005	801–898/1133–1301
SD16	4609	8.0	6.0	1400.0	19.0	377.0	<1	2640.0	159.0	4.7	0.70907	18.5	2001	915–1042/1280–1311
Averages	3927	12.8	5.8	1128.0	21.6	281.6	<1	2368.0	109.4	5.0	0.71041	20.4		
Doty Mountain Pod														
DP17	3118	9.6	3.4	905.1	10.7	305.4	<1	1884.2	ND†	5.3	0.71071	17.0	2007	1762–1931
DP18	2374	9.0	4.0	706.3	10.9	280.6	<1	1363.2	ND	4.1	0.71141	14.8	2007	2262–2403
DP19	4500	9.4	5.2	1395.8	15.7	308.5	<1	2765.5	ND	3.8	0.71090	19.7	2007	1481–1639
DP20	2514	11.7	8.1	661.9	16.4	37.9	<1	1778.1	ND	2.8	0.70896	15.2	2007	1328–1507
Averages	3127	9.9	5.2	917.3	13.4	233.1	<1	1947.8		4.0	0.71049	16.7		

*Water chemistry is reported in milligrams per liter.
**TDS = total dissolved solids.
†ND = no data available.

Table 2. Water Chemistry and Isotopic Analysis Data for Atlantic Rim Springs and Stream Samples

Sample Number	pH	Temperature (°C)	Water Chemistry*										Isotopic Analysis**	
			TDS†	Ca^{2+}	Mg^{2+}	Na^{+}	K^{+}	Cl^{-}	SO_4^{2-}	HCO_3^{-}	CO_3^{2-}	F^{-}	$^{87}Sr/^{86}Sr$	$\delta^{13}C_{DIC}$
Muddy Creek														
RFC30	8.0	8.5	411	71.3	11.1	12.4	3.1	6.8	92.8	214	<1	<0.1	0.71222	−7.6
RFC29	8.0	12.5	428	69.8	12.9	17.4	2.9	5.0	101.6	218	<1	<0.1	0.71202	−7.2
RFC31	7.9	12.4	426	58.6	16.1	24.1	2.9	5.4	120.4	198	<1	<0.1	0.71215	−7.4
RFC32	8.0	11.6	442	57.6	17.4	27.7	3.4	5.2	122.8	208	<1	<0.1	0.71152	−7.7
Averages	8.0	11.25	427	64.3	14.4	20.4	3.1	5.6	109.4	210	<1	<0.1	0.71198	−7.5
Mesaverde Group Springs														
RFC3	9.0	15.5	1271	<1	<1	373.0	2.0	7.0	4.0	818.0	67.0	8.0	0.71077	−9.3
RFC9	8.2	12.9	1667	207.0	128.0	91.0	11.0	15.0	788.0	427.0	<1	0.7	0.71145	−13.8
RFC11	8.6	12.3	886	23.0	15.0	215.0	3.0	3.0	198.0	427.6	<1	0.5	0.71115	−11.1
RFC12	8.3	14.8	1096	155.0	74.0	51.0	6.0	4.0	392.0	413.0	<1	0.3	0.71075	−10.1
RFC17	8.2	11.7	1082	66.0	34.0	214.0	4.0	3.0	387.0	372.6	<1	0.2	0.71103	−9.7
RFC19	7.3	ND	513	73.0	35.0	14.0	7.0	2.0	151.0	230.0	<1	0.3	0.71174	−14.9
RFC20	7.1	17.0	219	38.0	13.0	3.0	3.0	2.0	74.0	85.0	<1	<0.1	0.71077	−12.0
RFC6	ND††	ND	ND	ND	ND	ND	ND	ND	ND	ND	ND	ND	0.71144	−11.5
Averages	8.1	14.0	962	80.4	42.9	137.3	5.1	5.1	285	396	10.4	1.7	0.71114	−11.6
Steele Shale Springs														
RFC16	8.1	ND	1517	170.0	137.0	83.0	8.0	9.0	752.0	356.0	<1	<1	0.70969	−9.2
Sand Hill Springs														
SS1	8.0	8.5	683	75.0	39.0	45.0	3.0	1.0	78.0	441.0	<1	0.4	0.70934	−9.9
SS2	8.1	5.4	872	130.0	54.0	20.0	3.0	3.0	200.0	461.0	<1	0.3	0.70999	−8.7
SHO	8.3	5.8	540	73.0	33.0	8.0	13.0	4.0	54.0	354.0	<1	0.3	0.71012	−6.7
RFC13	8.1	12.9	639	100.0	41.0	6.0	2.0	2.0	113.0	374.0	<1	0.4	0.71005	−10.7
Averages	8.1	8.1	684	94.5	41.8	19.8	5.3	2.5	111	408	<1	0.4	0.70988	−9.0
Depleted Lewis Shale Springs														
RFC2	8.9	15.0	1214	1.0	<1	351.0	2.0	9.0	3	784.0	55.0	7.7	0.70868	−8.2
RFC5	8.9	16.9	1206	<1	<1	353.0	2.0	15.0	<1	775.7	1.9	0.3	0.70870	−6.6
RFC8	8.8	15.1	1238	<1	<1	352.0	2.0	9.0	2	848.0	16.0	7.2	0.70868	−7.6
RFC10	8.9	12.2	1174	1.0	<1	353.0	2.0	5.0	<1	747.2	55.0	8.7	0.70867	−7.1
RFC21	9.1	22.4	1049	3.0	1.0	301.0	3.0	2.0	<1	668.0	63.0	6.9	0.70911	−6.9
Averages	8.9	16.3	1176	1.4	1.0	342.0	2.2	8.0	2	765	38.2	6.2	0.70877	−7.3
Enriched Lewis Shale Springs														
JOR	ND	8.8	1170	2.0	0.5	349.0	4.0	7.0	1.0	752.0	50.0	4.8	0.71051	0.5
RFC23	8.8	ND	2376	22.0	74.0	519.0	7.0	69.0	330.0	1240.0	109.0	5.5	0.71003	3.6
SDS	8.7	10.5	1472	3.0	2.0	430.0	4.0	10.0	1.0	974.0	41.0	7.3	0.70887	−2.8
RFC4	ND	ND	1582	1.1	0.4	386.3	0.6	19.5	<1	1165.0	<1	9.0	0.70821	−1.4
RFC7	ND	ND	3774	3.0	5.0	1080.0	2.1	188.0	5.0	2420.0	61.0	8.0	0.70984	5.5
RFC24	ND	ND	4673	5.7	3.4	1714.4	8.2	685.2	<1	4256.9	86.0	<0.1	0.70885	13.3
Wild Cow	8.8	4.7	3425	3.0	3.0	1060.0	13.0	173.0	7.0	2030.0	127.0	8.7	0.70914	12.0
RFC1	8.5	15.6	2215	2	3	634.0	3.0	25.0	81.0	1410.0	52.0	5.2	0.70925	−3.1
RFC14	8.6	18.9	2748	5.0	1.0	813.0	9.0	2.1	1.0	1820.0	85.0	12.1	0.70908	5.4

Table 2. Continued

Sample Number	pH	Temperature (°C)	Water Chemistry*										Isotopic Analysis**	
			TDS†	Ca^{2+}	Mg^{2+}	Na^{+}	K^{+}	Cl^{-}	SO_4^{2-}	HCO_3^{-}	CO_3^{2-}	F^{-}	$^{87}Sr/^{86}Sr$	$\delta^{13}C_{DIC}$
RFC18	8.8	20.9	2693	<1	1.0	777.0	7.0	69.0	<1	1730.0	97.0	9.9	0.70912	5.5
DGS	8.7	7.7	2429	6.0	2.0	751.0	7.0	162.0	<1	1430.0	64.0	6.4	0.70993	8.0
DG1	8.7	3.8	2486	1.0	0.5	733.0	9.0	100.0	<1	1590.0	45.0	7.2	0.71020	7.5
DG2	8.7	4.1	2461	4.0	4.0	771.0	11.0	179.0	<1	1410.0	73.0	8.2	0.71014	7.7
DG3	8.8	6.7	2016	2.0	1.0	623.0	7.0	80.0	<1	1230.0	66.0	7.3	0.71053	6.1
RFC22	8.6	13.0	4673	7.0	4.0	1370.0	13.0	387.0	<1	2800.0	86.0	5.0	0.71010	6.9
RFC25	8.4	16.1	3134	4.0	2.0	906.0	7.0	201.0	<1	1970.0	38.0	5.3	0.70916	11.2
RFC26	9.0	16.9	4797	6.0	8.0	1400.0	15.0	324.0	57.0	2750.0	229.0	7.6	0.70933	5.1
RFC28	8.8	13.0	2502	<1	<1	668.0	11.0	83.0	4.0	1620.0	108.0	6.0	0.71025	2.0
RFC27	8.9	16.2	2032	1.0	<1	610.0	7.0	57.0	<1	1260.0	88.0	6.8	0.71043	6.3
Averages	8.7	11.8	2771	4.2	6.1	820.8	7.6	148.5	26.1	1782	79.2	7.2	0.70963	5.2

*Water chemistry is reported in milligrams per liter.
**$\delta^{13}C_{DIC}$ is in parts per thousand.
†TDS = total dissolved solids.
††ND = no data available.

with 1800 wells scheduled for completion (BLM, 2007). Currently, vertical wells are drilled on 80-ac spacing (BLM, 2007; WOGCC, 2010). Each well is cemented and cased and then perforated into the targeted coals within the Almond, Pine Ridge, or Allen Ridge formations. Some wells are stimulated with treated water and proppants or by fracture stimulation (WOGCC, 2010). The closed-completion style of Atlantic Rim CBNG wells is ideal for this study, as coproduced waters should originate from within the perforated coalbed reservoirs.

In the Atlantic Rim, CBNG production commences by drilling wells in close groupings, called "units" or "pods" (BLM, 2007). Water withdrawal from CBNG wells in pods lowers hydraulic pressure over a regional area, stimulating gas migration from the regional coal matrix. Most of the CBNG wells currently operating and scheduled for completion will be positioned on the Lewis Shale (Figure 1) (BLM, 2007). The total completed depths and target intervals of Atlantic Rim CBNG wells generally deepen to the west, and wells sampled for this study had completion depths that ranged between 801 and 2677 ft (244–816 m) below the surface.

METHODS

A total of 61 water samples were collected by the principal author and a BLM field hydrology crew and transported to the University of Wyoming in iced coolers. The 61 water samples collected for this study include surface water samples from 37 springs and seeps, four stream samples from Muddy Creek, and 20 samples from individual CBNG wellheads (Figure 1). Spring samples were collected during the summer and fall of 2006 and 2007, all Muddy Creek samples were collected on September 27, 2007, and all CBNG wells were sampled on May 15, 2007. Samples were filtered through a 0.45-μm pore diameter membrane filter, aliquoted, and prepared for analysis. Water chemistry analyses were completed at Inter-Mountain Laboratories in Sheridan, Wyoming, and at the University of Wyoming's geochemistry laboratory in the Department of Geology and Geophysics. Strontium isotopic analyses were completed at the University of Wyoming Radiogenic Isotope Laboratory in the Department of Geology and Geophysics. Carbon isotopic analyses were completed at the University of Wyoming Stable Isotope Facility. Production data for sampled CBNG wells, including total produced water

Table 3. CBNG Wells First 30 Months of Reported Water and Gas Production Data, along with $\delta^{13}C_{DIC}$ Values*

Area and Cumulative Data	Samples		Months 1	2	3	4	5	6	7	8	9	10	11	12	13	14	15	16
Brown Cow	**Average $\delta^{13}C_{DIC}$ = 2.2**																	
Water/Gas	BC1 (DIC = 1.1)	Gas	0	0	0	0	0	0	0	0	0	0	0	0	88	0	0	0
Ratio 3662		Water	12,710	16,020	18,600	14,260	19,500	7200	12,750	0	0	0	0	18,266	0	12,421	0	0
Total Water	BC2 (DIC = 3.9)	Gas	0	0	0	0	0	0	0	0	0	0	0	6	0	0	0	0
2,135,150		Water	4080	5766	23,157	0	14,304	27,300	0	0	0	0	27,857	0	9074	9613	7591	7693
Total Gas 583	BC3 (DIC = 0.6)	Gas	0	0	0	0	0	0	0	0	0	0	0	0	0	0	0	0
		Water	930	16,616	0	34,200	20,320	37,440	0	0	0	0	29,587	0	9428	10,050	9735	9904
	BC4 (DIC = 1.1)	Gas	0	0	0	0	0	0	0	0	0	0	0	0	0	0	0	0
		Water	17,608	18,570	35,030	36,580	41,400	15,200	28,050	0	0	0	0	16,826	0	0	0	0
	BC5 (DIC = 5.1)	Gas	0	0	0	0	0	0	0	0	0	0	0	0	0	0	0	0
		Water	11,656	14,550	25,451	18,445	27,000	0	0	0	0	0	0	0	0	0	0	0
	BC6 (DIC = 1.3)	Gas	0	0	0	0	0	0	0	0	0	0	0	0	0	0	0	0
		Water	1600	10,775	37,788	34,915	30,942	25,036	24,516	27,473	14,793	11,710	1696	17,224	27,347	27,719	25,409	32,018
Blue Sky	**Average $\delta^{13}C_{DIC}$ = 11.1**																	
Water/Gas	BS7 (DIC = 14.3)	Gas	0	0	1	0	0	0	0	0	0	10	86	26	12	57	11	49
Ratio 42		Water	52,140	65,159	66,609	48,123	26,148	43,504	53,936	30,236	61,130	75,217	70,931	83,758	94,008	87,698	0	111,741
Total Water	BS8 (DIC = 12.6)	Gas	36	218	59	711	215	124	484	74	52	135	315	32	71	17	22	32
4,181,799		Water	0	0	4834	4750	14,944	15,584	15,556	13,224	12,111	15,018	14,612	13,966	14,157	14,867	15,102	13,592
Total Gas	BS9 (DIC = 0.0)	Gas	0	886	758	1000	1815	835	2144	535	307	262	1399	1701	655	874	648	1336
98,899		Water	0	0	0	46,234	54,069	52,623	28,351	23,504	46,057	53,753	48,484	59,198	60,904	57,258	53,517	53,812
	BS10 (DIC = 18.8)	Gas	172	595	526	2214	373	677	674	202	144	385	459	116	117	189	212	345
		Water	0	0	46,236	24,836	11,040	29,749	25,274	27,084	30,215	32,461	30,712	35,268	34,543	32,748	34,001	33,000
	BS11 (DIC = 9.9)	Gas	117	264	284	215	218	175	556	124	141	495	376	57	60	73	93	174
		Water	0	0	21,952	30,303	25,920	24,872	25,043	25,751	28,839	27,924	29,918	27,971	25,709	25,972	21,500	25,763
Sun Dog	**Average $\delta^{13}C_{DIC}$ = 20.4**																	
Water/Gas	SD12 (DIC = 21.1)	Gas	4323	4934	3021	14,631	9389	3527	1506	0	0	25	428	2208	2228	2003	1631	3809
Ratio 6		Water	63,795	75,268	41,408	89,677	37,203	30,836	7779	0	0	0	55,537	20,329	0	59,619	0	86,098
Total Water	SD13 (DIC = 20.6)	Gas	2022	2657	3280	4756	6086	2379	3501	2180	922	1895	3530	4590	5350	5564	4399	6429
4,148,692		Water	34,080	48,759	27,815	29,308	33,003	25,167	30,696	0	0	0	36,786	8121	0	35,131	0	30,618

Total Gas	SD14 (DIC = 22.8)	Gas	2282	2221	3346	4373	5093	1568	2348	3393	2172	4251	5122	5114	4794	5097	4541	8088
695,475		Water	13,421	43,339	29,281	34,902	41,225	17,342	22,239	0	0	0	48,267	9412	0	39,318	0	39,492
	SD15 (DIC = 19.1)	Gas	3052	2828	2328	891	2818	2392	2703	1777	1550	2054	2408	2429	2228	2337	1985	2410
		Water	17,864	15,127	11,824	3445	12,597	12,114	12,250	0	0	0	16,905	3837	0	17,143	0	9906
	SD16 (DIC = 18.5)	Gas	1267	1702	1248	2308	2138	2319	3620	2240	847	3474	3082	4133	4852	4317	4159	4786
		Water	7102	12,089	6572	9110	7033	11,970	16,785	0	0	0	10,660	3509	0	18,381	0	18,374
Doty Mountain	**Average $\delta^{13}C_{DIC}$ = 16.7**																	
Water/Gas	DP17 (DIC = 17.0)	Gas	3	25	25	24	26	24	24	46	69	68	66	80	66	69	80	274
Ratio 15		Water	0	6037	3900	4696	5176	4227	5539	4068	4211	4366	4372	4253	7317	5674	5575	4064
Total Water	DP18 (DIC = 14.8)	Gas	24	25	24	26	24	24	23	23	23	22	6	15	23	27	1060	0
1,334,554		Water	16,503	7133	3900	4028	4104	4442	3967	4352	5046	5038	936	5896	10,836	16,103	20,431	26,766
Total Gas	DP19 (DIC = 19.7)	Gas	0	0	20	25	24	26	24	22	27	69	68	66	80	66	69	80
88,419		Water	1678	0	5627	6296	7005	6889	5368	4656	3879	5618	5581	5164	4949	7226	5898	5807
	DP20 (DIC = 15.2)	Gas	0	0	20	25	24	26	24	24	35	69	68	66	80	66	69	80
		Water	4965	0	11,166	10,286	13,959	12,275	6177	6859	9957	12,181	13,052	13,325	12,246	13,408	12,227	12,456

*Water is reported in barrels; gas is reported in thousand cubic feet; $\delta^{13}C_{DIC}$ values are in ‰. WOGCC (2010).

(reported in barrels [bbl]), gas (reported in mil (thousand) cubic feet [mcf]), depths of completion, location, and well history were downloaded from the WOGCC (2010) Web site. Cumulative water/gas ratios were determined by dividing total water (in bbl) by the total gas (in mcf) for the first 30 months of reported production. A structure contour map was created by downloading and picking Mesaverde Group formation tops from well logs of all available Atlantic Rim CBNG or traditional oil and gas wells (252 total wells downloaded from the WOGCC [2010] Web site). The coalbed reservoir enrichment map was created by interpolating $\delta^{13}C_{DIC}$ data through an inverse distance-weighted raster using Environmental Systems Research Institute (ESRI) spatial analysis software.

Geochemical Analysis

Anions were measured using ion chromatography. Cations were measured using the inductively coupled plasma mass spectrometric method. All cations, anions, calculated total dissolved solids (TDS), and alkalinity (as HCO_3^-) are recorded in milligrams per liter. Batch samples were processed in sets of 10 or 20, along with one spiked sample, one spike duplicate, and a secondary source control standard to ensure the reproducibility of quality control standards. Alkalinity was measured using acid-based titration methods.

Strontium Isotopic Analysis

Strontium was isolated from an unacidified sample using Teflon columns filled with Eichrom Sr-Spec resin, and the strontium isotopic composition was determined by thermal ionization mass spectrometry. The internal precision of $^{87}Sr/^{86}Sr$ isotopic measurements is ±0.00001. Analyses of the NBS 987 strontium standard measured during the course of this study gave an average value of $^{87}Sr/^{86}Sr$ = 0.71026 ± 0.00002 (2 standard deviations). Replicates show that $^{87}Sr/^{86}Sr$ values are reproducible within the uncertainty expected from the analysis of standard NBS-987. All analyses were normalized

Table 3. Continued

Area and Cumulative Data	Samples		Months 17	18	19	20	21	22	23	24	25	26	27	28	29	30	Total
Brown Cow	**Average $\delta^{13}C_{DIC}$ = 2.2**																
Water/Gas Ratio 3662	BC1 (DIC = 1.1)	Gas	0	0	0	0	0	0	0	0	0	0	0	0	0	0	88
		Water	0	0	2288	0	0	0	3418	0	1554	0	0	9554	19,546	16,209	184,296
Total Water 2,135,150	BC2 (DIC = 3.9)	Gas	0	0	0	0	0	0	0	0	0	0	0	0	0	0	6
		Water	7571	9516	12,130	12,325	8029	10,528	0	6203	20,109	31,821	33,214	33,923	19,756	15,854	357,414
Total Gas 583	BC3 (DIC = 0.6)	Gas	0	0	0	0	0	0	0	0	0	0	0	0	0	0	0
		Water	9930	9710	11,413	11,293	6464	9242	0	4921	23,792	39,595	43,720	38,037	21,290	243	407,860
	BC4 (DIC = 1.1)	Gas	0	0	0	0	0	0	0	0	0	0	0	0	0	0	0
		Water	0	0	909	0	0	0	0	0	0	11,552	35,544	43,428	43,333	27,984	372,014
	BC5 (DIC = 5.1)	Gas	0	0	0	0	0	0	0	0	0	0	0	0	0	0	0
		Water	0	0	0	0	0	0	0	0	0	4542	808	0	6247	4032	112,731
	BC6 (DIC = 1.3)	Gas	0	0	0	0	0	0	0	0	0	0	0	0	0	489	489
		Water	0	17,402	39,531	30,633	26,897	24,758	27,163	27,788	33,236	21,445	28,750	14,189	33,831	24,251	700,835
Blue Sky	**Average $\delta^{13}C_{DIC}$ = 11.1**																
Water/Gas Ratio 42	BS7 (DIC = 14.3)	Gas	423	139	154	210	470	1602	3408	3220	1836	1244	466	4127	5628	1501	24,680
		Water	79,739	85,590	0	69,773	56,156	0	33,546	33,182	23,353	8654	12,011	22,125	22,516	9917	1,426,900
Total Water 4,181,799	BS8 (DIC = 12.6)	Gas	27	98	90	60	68	83	97	68	101	61	64	67	40	82	3603
		Water	0	17,423	14,735	16,042	0	17,021	15,795	0	17,751	17,257	17,397	7086	6671	15,727	345,222
Total Gas 98,899	BS9 (DIC = 0.0)	Gas	1875	2118	4077	3224	3198	3660	3772	3784	2782	1299	1347	971	1110	275	48,647
		Water	57,074	0	55,027	46,055	47,003	0	56,859	55,204	0	44,700	50,521	34,131	24,330	14,848	1,123,516
	BS10 (DIC = 18.8)	Gas	240	600	300	225	862	802	759	515	293	323	312	419	145	196	13,391
		Water	0	32,080	18,188	12,458	0	28,568	22,823	0	41,916	33,332	27,268	14,649	10,853	6906	676,208
	BS11 (DIC = 9.9)	Gas	144	410	353	334	367	409	472	447	565	445	302	379	203	326	8578
		Water	0	28,824	25,007	25,165	0	31,554	25,953	0	19,996	17,976	15,632	20,082	12,250	20,077	609,953
Sun Dog	**Average $\delta^{13}C_{DIC}$ = 20.4**																
Water/Gas Ratio 6	SD12 (DIC = 21.1)	Gas	5231	3261	3508	2394	1058	2621	8292	8188	7193	7060	7169	4779	542	596	115,555
		Water	107,308	75,534	90,506	65,502	40,519	76,759	104,966	97,468	95,067	93,937	84,089	68,837	29,371	0	1,597,412
Total Water 4,148,692	SD13 (DIC = 20.6)	Gas	6952	4819	5944	8525	7287	7223	8056	8956	7867	8408	8747	7690	6222	7754	163,990
		Water	30,370	29,174	29,950	50,380	61,287	31,966	33,812	34,616	32,879	48,132	46,947	35,018	25,058	0	829,073
Total Gas 695,475	SD14 (DIC = 22.8)	Gas	7109	8224	10,561	12,786	9680	11,680	12,480	12,847	11,779	12,156	13,578	10,724	7031	12,121	216,559
		Water	53,281	54,360	59,024	56,499	50,553	55,327	66,991	61,644	32,863	25,683	53,757	39,318	25,715	0	973,253

	SD15 (DIC = 19.1)	Gas	2314	1905	2435	4899	2476	4412	4668	4714	3405	3404	3588	3068	2412	3494	83,384
		Water	10,392	9268	8508	8276	6093	22,006	30,348	32,856	26,954	28,314	28,104	24,578	21,476	0	390,185
	SD16 (DIC = 18.5)	Gas	4961	1978	1122	1580	4555	5640	5277	6297	5713	7110	7155	6086	5280	6741	115,987
		Water	19,485	16,657	9455	6833	21,173	24,305	23,074	19,254	16,586	25,179	17,789	19,787	17,607	0	358,769
Doty Mountain	**Average $\delta^{13}C_{DIC}$ = 16.7**																
Water/Gas	DP17 (DIC = 17.0)	Gas	0	0	0	0	0	0	93	87	25	0	14	0	163	368	1719
Ratio 15		Water	2272	2495	2347	2690	2054	1793	1936	1774	1501	1508	1861	3319	886	1310	101,221
Total Water	DP18 (DIC = 14.8)	Gas	0	67	254	341	855	342	262	304	985	1356	0	23	305	508	6971
1,334,554		Water	27,737	26,011	29,499	35,749	44,246	43,750	30,674	47,810	45,354	44,691	47,551	45,326	45,978	499	654,356
Total Gas	DP19 (DIC = 19.7)	Gas	0	0	0	0	0	0	0	22	99	3668	6630	3260	464	2124	16,933
88,419		Water	4412	4811	5014	4458	4825	3803	5058	1546	7588	41,455	16,039	3	0	19,800	200,453
	DP20 (DIC = 15.2)	Gas	1859	1800	1771	1687	1796	1692	1407	1222	2684	9527	6165	11,053	8323	11,134	62,796
		Water	10,513	12,872	11,420	10,730	11,837	10,550	6765	5392	13,657	37,702	11,015	27,962	20,053	23,517	378,524

*Water is reported in barrels; gas is reported in thousand cubic feet; $\delta^{13}C_{DIC}$ values are in ‰. WOGCC (2010).

to an $^{86}Sr/^{88}Sr$ value of 0.1194. Analytical blanks were less than 0.2 ng, negligible compared with sample sizes of at least 0.1 μg strontium. Strontium concentrations are reproducible at the 1% level.

Carbon Isotopic Analysis

For the analysis of dissolved inorganic carbon (DIC), samples were passed through a Cameo 0.45-μm nylon prefilter attached to a 60-mL Luer-Lok syringe. The filtered sample was transferred in 30-mL Wheaton glass serum vials with Teflon septa and crimp sealed with aluminum caps. Approximately 2 to 3 drops of benzalkonium chloride were added to each vial to halt metabolic activity. The $\delta^{13}C_{DIC}$ of samples was analyzed using a continuous-flow isotope ratio mass spectrometer system. This system comprises a GasBench-II device coupled to a Finnigan DELTA Plus mass spectrometer. The reproducibility and accuracy were monitored by replicate analysis of samples and internal laboratory standards and were more than ±0.1‰. The $\delta^{13}C_{DIC}$ values are reported in per mil relative to the Vienna Peedee Belemnite standard.

RESULTS

Data for well samples are presented in Table 1; geochemical and isotopic analyses for Atlantic Rim stream and spring samples are presented in Table 2; and production data for CBNG wells are presented in Table 3. Additional geochemical data, including minor ion concentrations and stable isotopic analysis of oxygen and deuterium, are available in McLaughlin (2009).

Muddy Creek Samples

Muddy Creek has Ca-HCO_3–type water chemistry (Figure 2; Table 2). The $^{87}Sr/^{86}Sr$ values from Muddy Creek samples have the highest values of all Atlantic Rim samples, ranging from 0.71152 to 0.71222 and averaging 0.71198 (Figure 3; Table 2). The $\delta^{13}C_{DIC}$ were negative, averaging –7.5‰ (Figure 4).

Figure 2. Trilinear plot of Atlantic Rim spring and stream samples. Two distinct populations are visible; those samples that are dominantly calcium-magnesium-sulfate or those that are dominantly sodium-bicarbonate. Data from Table 2.

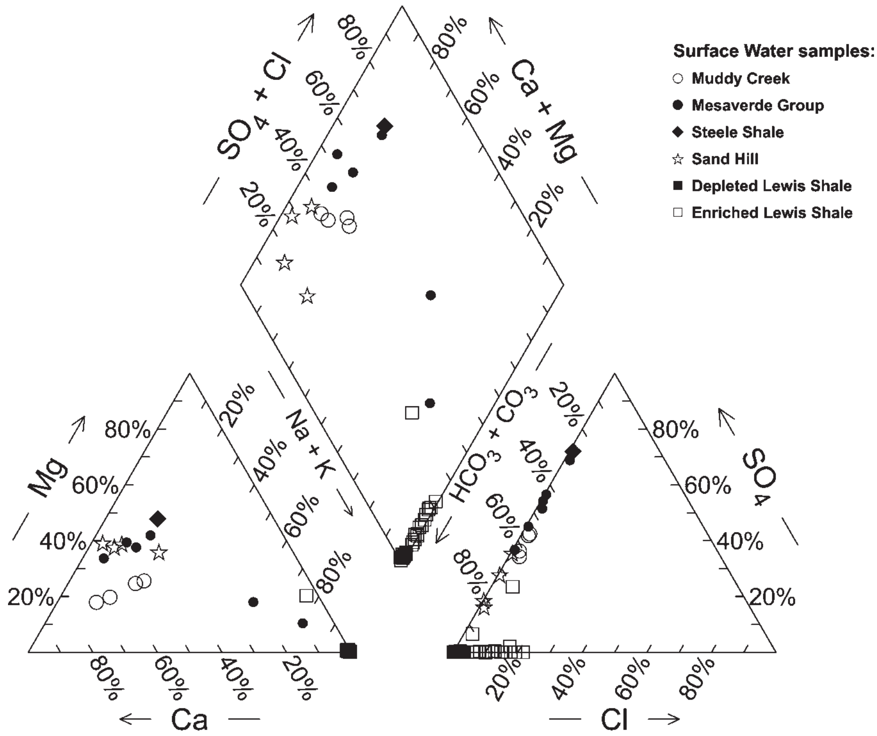

Atlantic Rim Spring Samples

Spring samples have been subdivided into Mesaverde Group, Lewis, Steele, and Sand Hill springs based on the geologic location of discharge, not the geologic unit from which they are sourced. This is especially pertinent for Lewis Shale springs, and these samples have been further subdivided based on whether they have depleted or enriched $\delta^{13}C_{DIC}$ values (which will be covered in detail in the Discussion). Some of the latter springs emit methane as well as water.

Mesaverde Group Springs

Most Mesaverde Group springs yielded Ca-Mg-SO_4–type water, whereas RFC11 and RFC17 have Na-SO_4-HCO_3–type waters and RFC3 has Na-HCO_3–type water (Figure 2; Table 2). Mesaverde

Figure 3. Strontium (Sr) isotopic compositions of stream, spring, and coal-bed natural gas (CBNG) well water samples. Data from Table 2.

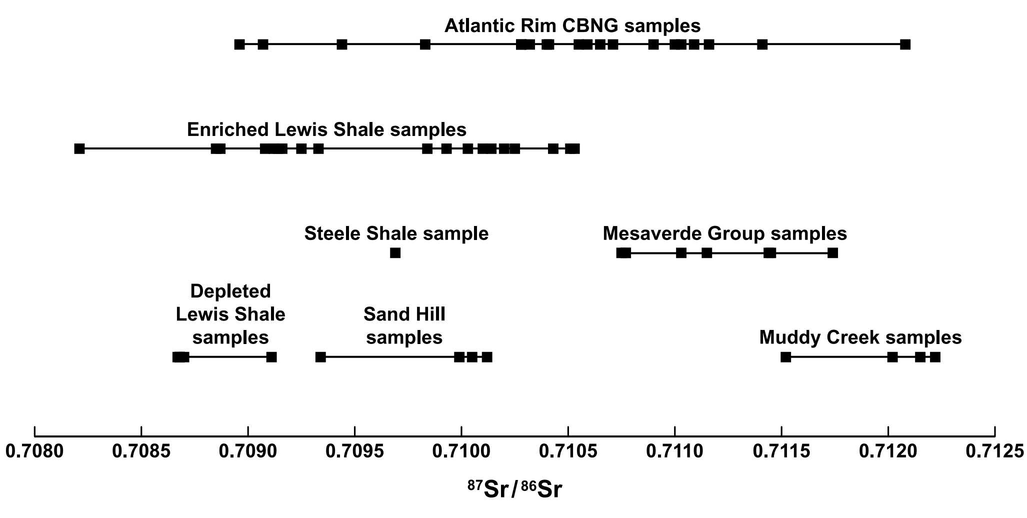

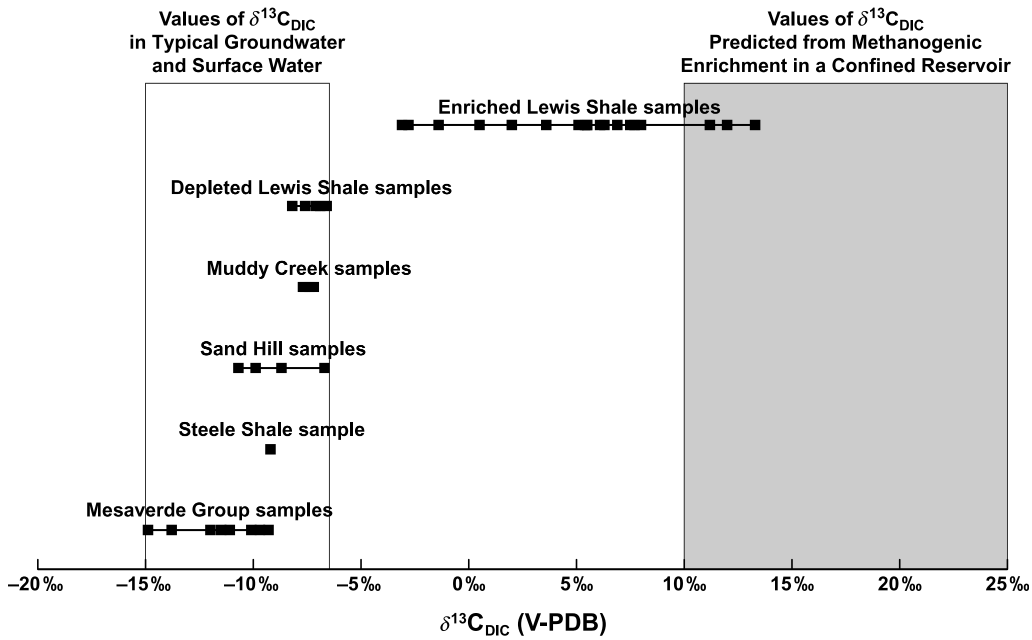

Figure 4. The range of $\delta^{13}C_{DIC}$ values of Atlantic Rim spring and stream samples. Unfilled box indicates typical values of $\delta^{13}C_{DIC}$ in Wyoming groundwater and surface water (Mook and Tan, 1991; Clark and Fritz, 1997; Sharma and Frost, 2008). Shaded box indicates predicted values of $\delta^{13}C_{DIC}$ by methanogenic enrichment in a confined reservoir (Simpkins and Parkin, 1993; Botz et al., 1996; Whiticar, 1999; Sharma and Frost, 2008). Data from Table 2. V-PDB = Vienna Peedee Belemnite.

Group springs have the highest $^{87}Sr/^{86}Sr$ of all spring samples, ranging from 0.71075 to 0.71174 and averaging 0.71114 (Figure 3; Table 2). Mesaverde Group springs have the lowest $\delta^{13}C_{DIC}$ of all samples, averaging –11.5‰ (Figure 4).

Steele Shale Springs

The Steele Shale spring has Ca-Mg-SO_4–type water chemistry (Figure 2; Table 2). $^{87}Sr/^{86}Sr$ is 0.70969 (Figure 3). The $\delta^{13}C_{DIC}$ value for the Steele Shale spring is negative, at –9.2‰ (Figure 4).

Sand Hill Springs

Sand Hill springs are primarily Ca-Mg-HCO_3–type water (Figure 2; Table 2). The $^{87}Sr/^{86}Sr$ values of Sand Hill springs range from 0.70934 to 0.71012 and averages 0.70988 (Figure 3). The $\delta^{13}C_{DIC}$ values were negative, averaging –9.0‰ (Figure 4).

Depleted Lewis Shale Springs

All Lewis Shale springs yield Na-HCO_3–type waters (Figure 2; Table 2). The five depleted Lewis Shale spring samples with negative $\delta^{13}C_{DIC}$ (within the range of typical groundwater) have the lowest $^{87}Sr/^{86}Sr$ of all spring samples, ranging from 0.70867 to 0.70911 and averaging 0.70877 (Figure 3). The $\delta^{13}C_{DIC}$ values were negative, averaging –7.3‰ (Figure 4).

Enriched Lewis Shale Springs

Nineteen of the sampled springs from the Lewis Shale have $\delta^{13}C_{DIC}$ values that are higher than expected for typical groundwater (Figure 4). Among these are 13 samples from springs that were observed to bubble methane. The $\delta^{13}C_{DIC}$ were mostly positive, averaging +5.2‰, and are the highest $\delta^{13}C_{DIC}$ of all Atlantic Rim springs (Figure 4; Table 2). Enriched Lewis Shale springs emit Na-HCO_3–type waters and have $^{87}Sr/^{86}Sr$ values that range from 0.70821 to 0.71053 and average 0.70963 (Figure 3; Table 2).

Coalbed Natural Gas–Produced Water

Samples from Atlantic Rim CBNG wells have Na-HCO_3–type waters (Figure 5; Table 1). The $^{87}Sr/^{86}Sr$ values of CBNG wells range from 0.70896 to 0.71208 (Figure 3). The $\delta^{13}C_{DIC}$ values were positive, ranging from +0.0 to +22.8‰ (Figure 6). Sun Dog wells have the highest average $\delta^{13}C_{DIC}$

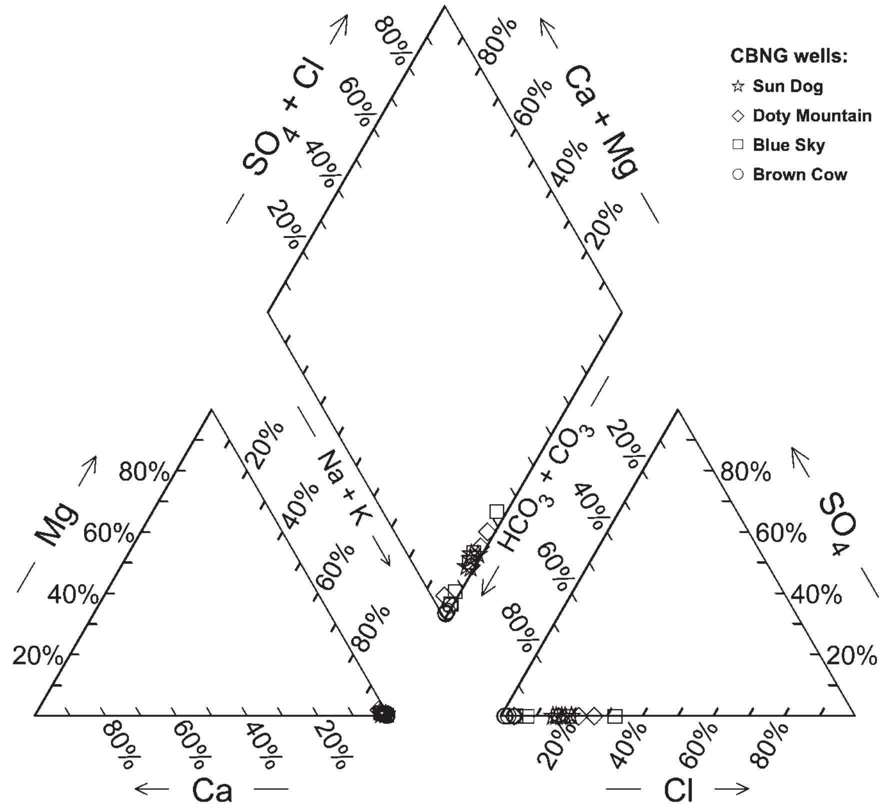

Figure 5. Piper diagram of Atlantic Rim CBNG samples. Data from Table 1.

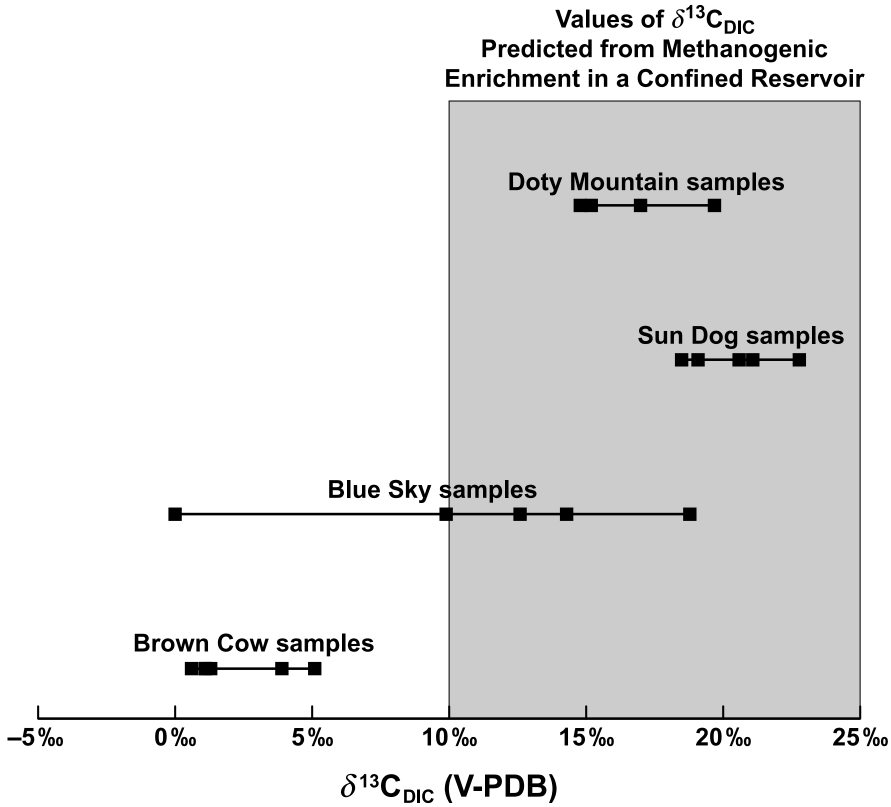

Figure 6. Range of $^{13}C_{DIC}$ for CBNG wells by pod. Shaded box indicates predicted values of $\delta^{13}C_{DIC}$ by methanogenic enrichment in a confined reservoir (Simpkins and Parkin, 1993; Botz et al., 1996; Sharma and Frost, 2008). Data from Table 1. V-PDB = Vienna Peedee Belemnite.

of +20.4‰, and Brown Cow wells have the lowest average $\delta^{13}C_{DIC}$ of +2.1‰. Of the samples from the Blue Sky pod, sample BS9 has the lowest $\delta^{13}C_{DIC}$ of +0.0‰.

DISCUSSION

Geochemical and Isotopic Characterization of the Surface Water and Groundwater of the Atlantic Rim

The initial motivation for this study was to perform a baseline characterization of the surface water and groundwater in the study area, against which any changes related to CBNG development could be assessed. Water chemistry, strontium isotopic ratios, and the carbon isotope signature of dissolved organic carbon were chosen as suitable parameters for this characterization for the reasons subsequently discussed.

Water Chemistry

The CBNG waters from nonmarine deposits in Wyoming have distinctive Na-HCO_3–type water chemistry (Van Voast, 2003; Brinck et al., 2008). The CBNG waters from deep basins and/or marine deposits, like those of the Atlantic Rim, commonly contain a mix of Na-HCO_3 and Na-Cl–type waters (Pashin et al., 1991; Ayers and Kaiser, 1994; Pashin, 2007; McLaughlin, 2009). Regardless of sediment type, fully established CBNG waters are defined by the geochemical reactions and methanogenic-related biological processes that effectively eliminate calcium, magnesium, and sulfate, and increase the concentrations of dissolved CO_2 and sodium (Van Voast, 2003; Brinck et al., 2008). Groundwater and surface water not associated with CBNG can have a wide range of water chemistry compositions, which is seen in the aquifers of Carbon County, Wyoming (Clarke, 1916; Van Voast, 2003; Bartos et al., 2006).

Strontium Isotopes

Natural waters acquire strontium by dissolution of minerals or ion exchange reactions on mineral and rock surfaces; hence, strontium isotopic ratios represent a record of water-rock interaction (Collerson et al., 1988; Banner et al., 1994; Frost and Toner, 2004). Variations in $^{87}Sr/^{86}Sr$ of surface water and groundwaters reflect natural variations in the composition of geologic materials with which they interact. Isotopic variations arise because of radiometric decay of ^{87}Rb to ^{87}Sr (half-life, 48.8 billion yr). Rocks and minerals that have high Rb/Sr ratios will develop higher $^{87}Sr/^{86}Sr$ with time; rocks and minerals that are younger, or have low Rb/Sr ratios, will have lower $^{87}Sr/^{86}Sr$. The $^{87}Sr/^{86}Sr$ of groundwater is not affected by evaporative fractionation or directly by precipitation, and the precision of the $^{87}Sr/^{86}Sr$ analysis (±0.00001) allows for the detection of small variations in surface water and groundwater composition (Frost and Toner, 2004).

Carbon Isotopes

Dissolved inorganic carbon is the primary inorganic form of carbon in most natural waters and is composed of three major species: H_2CO_3, HCO_3^-, and CO_3^{2-} (Clark and Fritz, 1997). The two primary sources of DIC in natural waters are CO_2 derived from decaying organic matter and carbonate rock dissolution (the contribution of atmospheric CO_2 being negligibly small) (Mook and Tan, 1991; Clark and Fritz, 1997). The averages of the two contributing end members, that is, soil CO_2 and carbonate rocks, are approximately −25 and 0‰, respectively. In a moderately vegetated temperate drainage such as that found in Wyoming, $\delta^{13}C_{DIC}$ values in typical groundwater and surface water range from approximately −7 to −14‰ (Figure 3) (Mook and Tan, 1991; Clark and Fritz, 1997; Sharma and Frost, 2008; McLaughlin, 2009).

Highly enriched $\delta^{13}C_{DIC}$ values of +10 to +30‰ are documented only in reduced, organic-rich, hydraulically confined reservoirs where bacterial methanogenesis continually fractionates DIC species via acetate fermentation ($CH_3COOH \rightarrow CH_4 + CO_2$) and/or CO_2 reduction ($CO_2 + 4H_2 \rightarrow CH_4 + 2H_2O$) (Simpkins and Parkin, 1993; Scott et al., 1994; Botz et al., 1996; Martini et al., 1998; Whiticar, 1999; Hellings et al., 2000; Aravena et al., 2003; Pitman et al., 2003; McIntosh et al., 2008; Sharma and Frost, 2008). The process of $\delta^{13}C_{DIC}$ enrichment is well recognized in CBNG reservoirs. Highly enriched carbon ratios, attributed to increased activity levels of bacterial methanogenesis within the reservoir, were recorded in bituminous Pennsylvanian coals in the Black Warrior Basin, Alabama (Pitman et al., 2003). Enriched $\delta^{13}C_{DIC}$ values between +2.8 and +13.1‰ were measured in CBNG water samples from Pennsylvanian bituminous coals in the Forest City Basin, Kansas (McIntosh et al., 2008). In Wyoming, CBNG water samples from subbituminous Tertiary coals in the Powder River Basin have enriched $\delta^{13}C_{DIC}$ values of +12 to +22‰ (Sharma and Frost, 2008).

Stream Samples

Because precipitation has very low strontium contents, most of the strontium in surface waters is acquired through interaction with soil and rock (Frost and Toner, 2004). Therefore, the $^{87}Sr/^{86}Sr$ of Muddy Creek samples reflects interaction with geologic materials in the drainage. Precambrian granites and gneisses from the western slope of the Sierra Madre have present-day $^{87}Sr/^{86}Sr$ values that range between 0.71725 and 0.93989 (Souders and Frost, 2006). The high $^{87}Sr/^{86}Sr$ of Muddy Creek samples indicates an influence from these Precambrian rocks. As Muddy Creek traverses Cretaceous outcrops, the $^{87}Sr/^{86}Sr$ of the samples becomes progressively lower both because of interaction with less radiogenic minerals and by input of groundwater with relatively low $^{87}Sr/^{86}Sr$. This is illustrated by Mesaverde Group spring sample RFC17, which enters Muddy Creek downstream from RFC30 and contributes a lower $^{87}Sr/^{86}Sr$ value to the stream (Figure 1; Table 2).

The $\delta^{13}C_{DIC}$ values of Muddy Creek samples are negative, averaging −7.5‰, within the range of typical groundwater and surface water found in Wyoming. Low $\delta^{13}C_{DIC}$, TDS, and the Ca-HCO_3–type water chemistry of Muddy Creek suggest no influence of methanogenically enriched water (Table 2).

Mesaverde Group Springs

Relative to other Atlantic Rim springs, Mesaverde Group spring waters are distinguished by high $^{87}Sr/^{86}Sr$, similar to Muddy Creek samples (Figure 3). Water with high $^{87}Sr/^{86}Sr$ from Sierra Madre–sourced drainages and creeks, like that in Muddy Creek, infiltrate and recharge reservoirs in the Mesaverde Group. Geochemical characteristics of Mesaverde Group springs suggest a relatively short groundwater residence time, such that limited introduction of unradiogenic $^{87}Sr/^{86}Sr$ from reservoir minerals and insufficient transit time for sulfate reduction and acquisition of sodium for most samples occurred.

The $\delta^{13}C_{DIC}$ values of the Mesaverde Group springs sampled are negative, averaging −11.6‰, indicating that no influence of methanogenically enriched water (Figure 4). This is corroborated in the water chemistry of Mesaverde Group springs, which are primarily Ca-Mg-SO_4–type water, a composition which is atypical of CBNG-produced water (Van Voast, 2003; Brinck et al., 2008). Mesaverde Group spring RCF3 is an exception because RFC3 has Na-HCO_3–type water nearly devoid of Ca-Mg-SO_4, a characteristic of geochemically evolved Atlantic Rim CBNG-produced waters and depleted and enriched Lewis Shale springs. The $\delta^{13}C_{DIC}$ of RFC3 is −9.3‰, more enriched than other Mesaverde Group spring samples (Table 2). The RFC3 sample is located less than 1000 ft (305 m) from three depleted Lewis Shale springs near the contact of the Mesaverde Group and the Lewis Shale (Figure 1). Although radiogenic $^{87}Sr/^{86}Sr$ of RFC3 is comparable to other Mesaverde Group springs (0.71077), its geochemical properties are most similar to the evolved water of adjacent depleted Lewis Shale springs (Figure 2; Table 2). RFC11 and RFC17 are primarily Na-HCO_3 but still contain Ca-Mg-SO_4, indicating that they have experienced geochemical evolution, although to a lesser degree than RFC3 (Figure 2; Table 2).

Steele Shale Spring

The Steele Shale spring is located near the headwaters of Cow Creek, close to the contact of the Steele Shale and Mesaverde Group (Figure 1). The negative $\delta^{13}C_{DIC}$ value (−9.2‰) of the Steele Shale spring, along with a Ca-Mg-HCO_3–type water chemistry, indicates that no influence of methanogenically enriched water occurs (Figures 2, 4). Its $^{87}Sr/^{86}Sr$ value (0.70969; Table 2; Figure 3) falls between the range of Mesaverde Group and depleted

Lewis Shale springs and may reflect introduction of minerals with low $^{87}Sr/^{86}Sr$ from the shale.

Sand Hill Springs

The unconsolidated eolian material of the Sand Hills has a high permeability, and recharge is likely a combination of direct infiltration of meteoric waters and discharge from the underlying Lewis Shale and/or Mesaverde Group reservoirs. Four Sand Hill springs were sampled: two samples (SHO and RFC13) from the interior of the dune field and two samples (SS1 and SS2) at the base of the dune field (Figure 1).

Sand Hill springs have intermediate $^{87}Sr/^{86}Sr$ values relative to Mesaverde Group and Lewis Shale springs, possibly indicating a contribution of strontium from both of these formations, or as a result of the foreign wind-blown minerals that constitute the dunes (Figure 3).

The $\delta^{13}C_{DIC}$ of Sand Hill springs is negative, indicating little or no influence from methanogenically enriched water (Figure 4; Table 2). Sand Hill springs have Ca-Mg-SO_4–type water, similar in composition to Mesaverde Group springs but with lower sodium, chloride, and sulfate, possibly indicating dilution by precipitation (Table 2).

Depleted Lewis Shale Springs

Depleted Lewis Shale springs were sampled in the southern part of the study area, approximately 1.9 mi (3 km) from the Brown Cow pod (Figure 1). The $\delta^{13}C_{DIC}$ values of depleted Lewis Shale springs are negative and reflect values expected of typical groundwater. Depleted Lewis Shale springs are defined by low $^{87}Sr/^{86}Sr$ values, from 0.70867 to 0.70911, which suggests a flow path through soils and rock that differs from the flow path of high $^{87}Sr/^{86}Sr$ waters that feed Mesaverde Group springs (Figure 3; Table 2). The Na-HCO_3 composition of all Lewis Shale springs suggests that the water has a sufficiently long subsurface residence time, during which sulfate reduction has occurred and calcium and magnesium have precipitated.

Enriched Lewis Shale Springs

The carbon isotope signatures of enriched Lewis Shale springs are elevated relative to typical groundwater values, averaging +5.2‰ (Figure 4; Table 2). This indicates that water feeding enriched Lewis Shale springs has undergone enrichment by methanogenic bacteria, which is consistent with the presence of methane that is discharged from some of these springs (Figure 4).

The carbon isotopic enrichment of the water in these springs could have occurred in either of two reservoirs: in the organic-rich coal beds of the underlying Mesaverde Group or within organic-rich strata of the Lewis Shale itself. The Mesaverde Group source is more likely for several reasons. Enriched Lewis Shale springs have a Na-HCO_3–type water composition and high levels of TDS, sodium, chloride, and bicarbonate that are similar to Mesaverde Group CBNG samples (Figures 2, 5; Tables 1, 2). Enriched Lewis Shale springs have highly variable $^{87}Sr/^{86}Sr$ values as do Atlantic Rim CBNG wells (Figure 3; Tables 1, 2). These springs are located at, or near, subsurface Mesaverde Group structural highs and/or faults and in topographic lows hosting drainages, mostly along Cow Creek and Wild Cow Creek (Figure 1). They are located near the contact between the Lewis Shale and the Mesaverde Group in places where the Lewis Shale is relatively thin (Figure 1). Nearby outcrops of competent Mesaverde Group sandstone rise up to several hundred feet above the soft truncated shale of the Lewis Shale. The geochemical characteristics, structural relationship, and hydrologic gradient between the formations suggest that enriched Lewis Shale springs are the surface expression of groundwater sourced within Mesaverde Group reservoirs. However, geochemical, structural, and topographic relationships are not the only evidence for the source of enriched Lewis Shale springs.

Both depleted and enriched Lewis Shale springs were sampled from the base of the Lewis formation, which has a low capacity for migrating fluids and is an unlikely reservoir to continuously accumulate and discharge groundwater and methane gas (Figure 1) (Roehler, 1990; Hettinger and Roberts, 2005; Bartos et al., 2006). Furthermore, both depleted and enriched Lewis Shale springs were sampled from similar lithologies within the stratigraphic base of the formation, but only one set of springs indicated enrichment by methanogenic bacteria (Figure 4; Table 2). This either indicates that fluids in the Lewis Shale are subjected to an undefined heterogeneous process of preferential carbon isotope enrichment, or that they were enriched in a different organic-rich reservoir and have migrated.

The geochemical characteristics, natural hydrologic gradient and structural relationships, existence of springs emitting water and gas in a formation with a low capacity for fluid transmission, and presence of springs in the Lewis Shale that are both depleted and enriched in isotopes of DIC all suggest that fluids emanating from enriched Lewis Shale springs do not originate within the Lewis Shale, but instead are sourced, at least in part, from coalbed reservoirs in the underlying Mesaverde Group. These same data also suggest that depleted Lewis Shale springs are sourced from Mesaverde Group reservoirs, although from reservoirs that are not methanogenically enriched. Mesaverde Group spring sample RFC3 is both proximal and geochemically similar to depleted Lewis Shale springs and represents water from a Mesaverde reservoir that likely supplies depleted Lewis Shale springs (Table 2).

Regarding the source of the gas in enriched Lewis Shale springs, methanogenic processes in local Mesaverde Group coal beds both enrich the carbon isotopic composition of the water and also emplace methane into the reservoir. The local underlying Mesaverde CBNG reservoir may be influenced by natural variations in near-surface hydraulic pressures, resulting in the desorption of the gas from the coal bed and migration and discharge of the gas through existing flow paths.

Synopsis of Atlantic Rim Springs

Atlantic Rim springs with radiogenic strontium and Ca-Mg-SO_4–type major ion chemistry identify water that has not undergone sulfate reduction and is therefore relatively young (Brinck et al., 2008). Spring water with unradiogenic strontium and Na-HCO_3–type major ion chemistry emerges from the Lewis Shale in the southern part of the study area, indicating that these springs are fed by more geochemically evolved water that has undergone sulfate reduction. Enriched Lewis Shale water has Na-HCO_3–type major ion chemistry and more radiogenic strontium ratios.

Most Atlantic Rim springs have $\delta^{13}C_{DIC}$ values that fall within the range of typical groundwater and surface water and record normal geochemical interactions and processes. Enriched Lewis Shale springs are an exception as they have $\delta^{13}C_{DIC}$ values indicative of enrichment by bacterial methanogenesis (Figure 4).

Actively bubbling methane springs are likely sourced from Mesaverde Group coalbed reservoirs. The amount of methane emitted from these springs fluctuates; the principal author observed various amounts of gas, from zero gas emissions to a "rolling boil," discharging from the same spring during multiple visits for two field seasons. The variability of gas emissions may be related to local variations in hydrostatic pressure of near-surface coalbed reservoirs or the variability of gas influx from saturated reservoirs. Because fluids feeding these springs are at least partially sourced from Mesaverde Group coalbed reservoirs, enriched $\delta^{13}C_{DIC}$ springs could potentially be influenced by CBNG production.

The Application of $\delta^{13}C_{DIC}$ for Characterizing Coalbed Natural Gas Reservoirs

The second goal of this study was to determine the extent to which carbon isotopic tracers in produced water can guide CBNG development to those areas where gas production is maximized and water production is minimized. Positive $\delta^{13}C_{DIC}$ of CBNG-produced water indicates that bacterial methanogenesis is associated with these waters (Figure 6; Table 1). However, a significant range in $\delta^{13}C_{DIC}$ exists in Atlantic Rim CBNG samples, which provides additional information about the potential for CBNG production from individual wells and related reservoirs (Figure 6).

Theoretically, because CBNG production targets the same Mesaverde Group coal beds reservoirs across the Atlantic Rim, the $\delta^{13}C_{DIC}$ values of produced waters should be comparable that is to say, Mesaverde Group coal beds that correlate stratigraphically and have similar depths and structural settings should result in reservoirs wherein coalbed water has undergone similar $\delta^{13}C_{DIC}$ enrichment. This is not the case in Mesaverde Group coalbed water (Figure 6; Table 1). Most noticeably, all CBNG wells from the Brown Cow pod have relatively low $\delta^{13}C_{DIC}$ (Figure 6; Table 1). Wells from the Blue Sky pod have a high relative variability of carbon enrichment: peripheral wells BS7 and BS10 are more enriched than wells in the center of the pod (BS8, BS9, and BS11) (Figure 6; Table 1). This indicates that water from coalbed reservoirs of the Brown Cow and some Blue Sky wells, although enriched compared with typical depleted groundwater, are either associated with less active methanogenic bacteria than other Atlantic Rim CBNG samples or these samples have been diluted with light depleted $\delta^{13}C_{DIC}$ water. If dilution is the explanation for the low $\delta^{13}C_{DIC}$ of these samples, then applying a simple binary mixing calculation using enriched $\delta^{13}C_{DIC}$ from Sun Dog wells and depleted $\delta^{13}C_{DIC}$ from Mesaverde Group springs suggests that the proportion of depleted $\delta^{13}C_{DIC}$ water produced from these wells is approximately between one-half and three-fourths.

In addition to the lower $\delta^{13}C_{DIC}$ values, the water chemistry of Brown Cow, BS8, BS9, and BS11 samples differs from other produced water samples (Figure 5; Table 1). The TDS content is lower, and bicarbonate, chlorine, and sodium concentrations in these wells are more similar to Atlantic Rim springs than to other produced water samples (Tables 1, 2). The lower $\delta^{13}C_{DIC}$ and water chemistry values of Brown Cow wells, BS8, BS9, and BS11 suggest the influence of a hydraulic connection to other depleted groundwater or surface water sources.

Structural analysis of the Mesaverde Group in the subsurface indicates that the reservoirs of Atlantic Rim CBNG wells with relatively low $\delta^{13}C_{DIC}$ have been influenced by faulting and fracture systems. An unsealed fault in the subsurface can create a pathway for fluid migration. Although no mapped surface expressions of faulting in the area of the Brown Cow and Blue Sky wells exist (Figure 1), a subsurface structure contour map of the Mesaverde Group identifies multiple faults, the largest being a normal fault located just west of sampled Brown Cow wells (Figure 8). This fault has nearly 1000 ft (305 m) of vertical throw and has offset Mesaverde Group coalbed reservoirs, providing the mechanics for an unconfined hydrologic system. If the fault is nonsealing, it may provide a pathway for isotopically depleted water to migrate into the reservoir from above or below, resulting in samples that have less brine and a lessened methanogenic carbon isotope signature (Figure 7C).

Unlike Brown Cow wells, all of which have comparable water characteristics, samples at the center of the Blue Sky pod are isotopically and chemically distinct from the water of peripheral Blue Sky wells (Figure 1; Table 1). The structure contour map identifies two faults striking north-south through the center of the sampled Blue Sky wells, which become progressively enriched with regard to $\delta^{13}C_{DIC}$ the farther they are positioned from the faults (Figures 1, 7B, 8). Well BS9, located between the faults at the center of the Blue Sky pod, has a $\delta^{13}C_{DIC}$ of +0.0‰, whereas wells to the east and the west of the fault have enriched $\delta^{13}C_{DIC}$ of +14.3 and +18.8‰, respectively (Figure 7B; Table 1). Analyte concentrations also increase with distance from these faults (Table 1). This suggests that CBNG reservoirs in the Blue Sky pod are partially confined or unconfined as a result of faulting (Figure 7B), allowing water with isotopically light carbon compositions and lesser amounts of brine to mix into the coalbed reservoir.

Although samples in the Doty Mountain and Sun Dog pods do not have the degree of isotopic variation recorded in Brown Cow and Blue Sky wells, evidence exists that $\delta^{13}C_{DIC}$ values in these pods also define attributes related to hydraulic confinement. Analysis of $\delta^{13}C_{DIC}$ values in Doty Mountain wells and the structure contour map indicate that the coalbed reservoirs of sample DP18 could be partially confined or unconfined as a result of faulting. The deepest sampled well in the pod, DP18 has the lowest measured $\delta^{13}C_{DIC}$ value of all Doty Mountain wells and is located less than 250 ft (76 m) from a fault (Figure 8; Table 1). When compared with the nearest Doty Mountain wells, the lower $\delta^{13}C_{DIC}$ values, as well as lesser concentrations of analytes, of DP18 suggest that water with isotopically light carbon compositions and lesser amounts

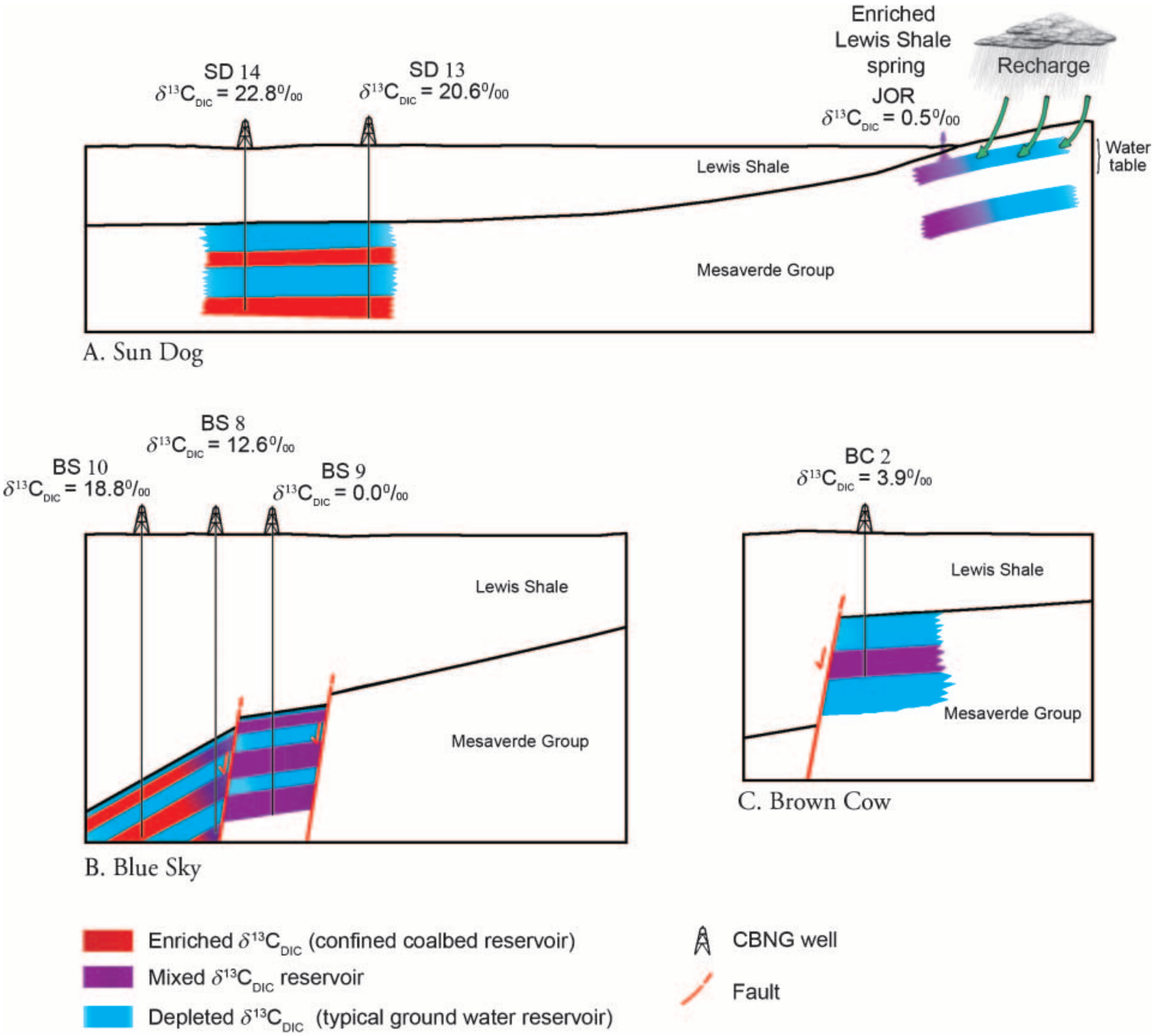

Figure 7. Schematic diagrams illustrating reservoir systems and associated $\delta^{13}C_{DIC}$ enrichment of Atlantic Rim coalbed reservoirs. Panel A illustrates highly enriched confined coalbed reservoirs of Sun Dog wells and shows the influence of recharge and near-surface reservoirs on $\delta^{13}C_{DIC}$ of enriched Lewis Shale spring JOR. Panel B illustrates fault-related partially confined coalbed reservoirs of variably enriched Blue Sky wells. Panel C illustrates fault-related partially confined coalbed reservoirs of low $\delta^{13}C_{DIC}$ Brown Cow wells. Data from Table 1.

of brine has been introduced into the coalbed reservoir, possibly along the fault (Figure 8; Table 1).

All Sun Dog wells are isotopically enriched with regard to carbon relative to most other Atlantic Rim wells (Figure 6; Table 1). Sun Dog wells are located on the crest of a broad anticline and are not associated with any faults (Figures 7A, 8). Although Sun Dog wells are completed at similar depths and intervals to Brown Cow wells, they have much higher $\delta^{13}C_{DIC}$ values and analyte concentrations (Table 1). This suggests that Sun Dog coalbed reservoirs have not mixed with isotopically light lower brine water, and that these reservoirs are nearly or wholly confined (Figure 7A).

The Application of $\delta^{13}C_{DIC}$ for Analyzing Coalbed Natural Gas Production Potential

We have suggested that $\delta^{13}C_{DIC}$ in Atlantic Rim CBNG wells can be used to indentify hydraulically confined CBNG reservoirs. This capability alone makes $\delta^{13}C_{DIC}$ a significant coalbed reservoir and

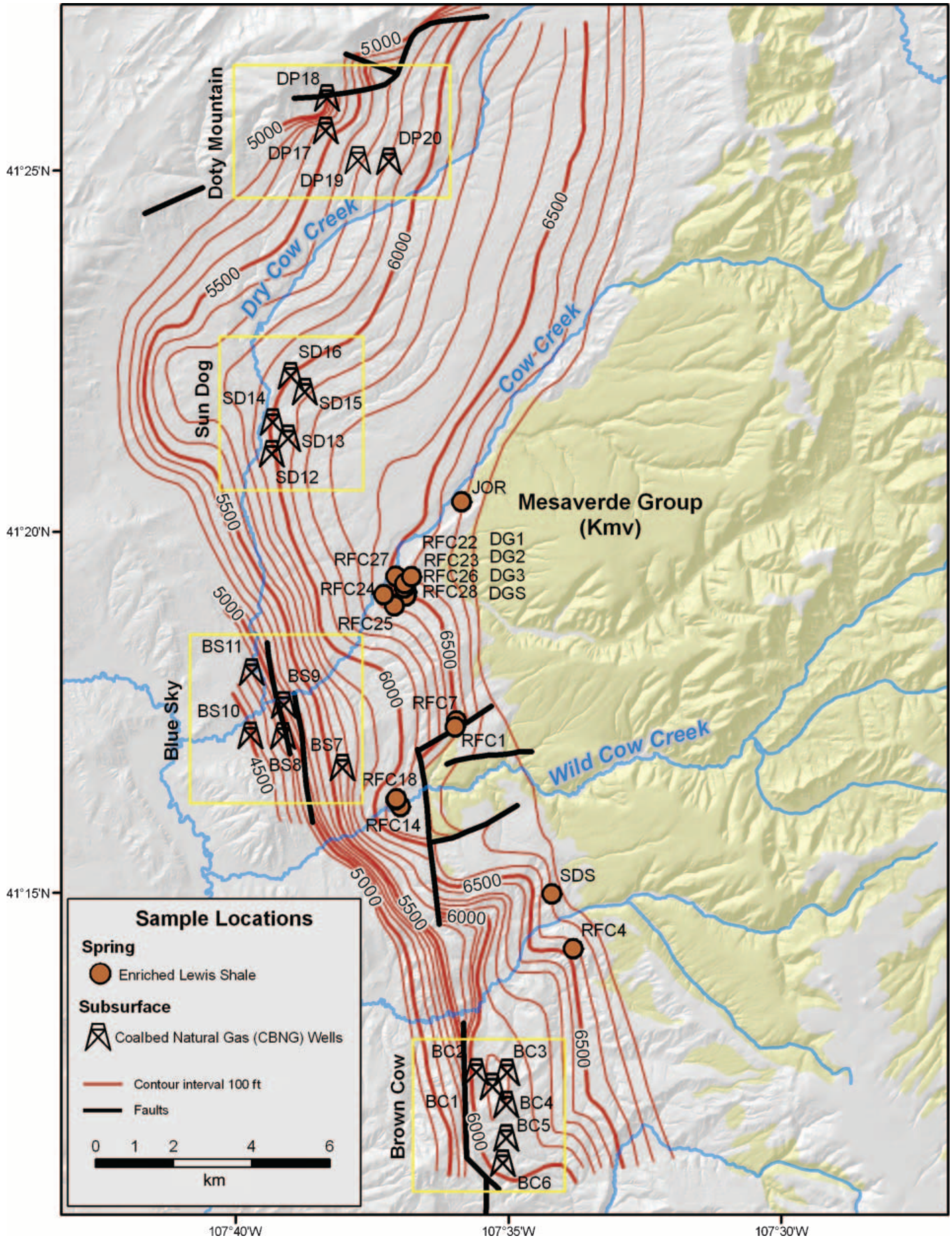

Figure 8. Structure contour map of the top of the Mesaverde Group (elevation above sea level). Contour intervals equal 100 ft (30.5 m) (WOGCC, 2010).

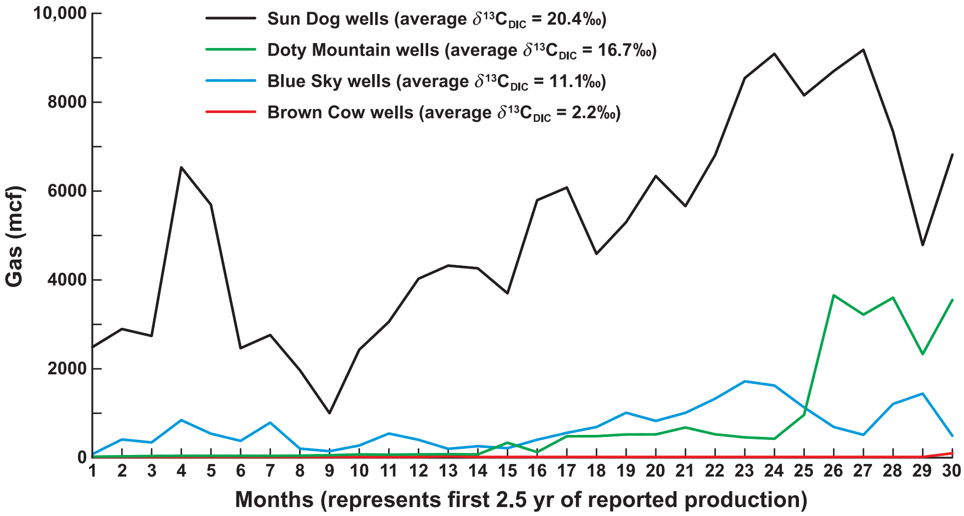

Figure 9. The average monthly gas produced for all sampled coalbed natural gas (CBNG) wells by pod for the first 30 months of reported production (WOGCC, 2010). Data from Table 3.

CBNG analysis tool, but further evidence suggests that $\delta^{13}C_{DIC}$ analysis can be applied to help evaluate the production potential of a CBNG field like the Atlantic Rim.

Atlantic Rim CBNG wells record a correlation of the amount of produced gas with $\delta^{13}C_{DIC}$ (Figure 9; Table 3). Gas production was analyzed for the first 30 months of reported data for each Atlantic Rim CBNG well sample (Table 3). Sun Dog well samples have the highest $\delta^{13}C_{DIC}$ and produced the most gas, whereas Brown Cow well samples have the lowest $\delta^{13}C_{DIC}$ and produced little or no gas (Figure 9; Table 3). Figure 9 shows that Sun Dog wells and most Blue Sky wells generate gas immediately after water production begins, although the low $\delta^{13}C_{DIC}$ Blue Sky wells have produced less gas than high $\delta^{13}C_{DIC}$ Sun Dog wells. Unlike Sun Dog and Blue Sky wells, most Doty Mountain wells do not generate gas immediately. However, they do produce more gas than Blue Sky wells after 24 months, indicating that with time, the hydraulic pressure of Doty Mountain CBNG reservoirs can be effectively lowered to promote the desorption of gas (Figure 9; Table 3).

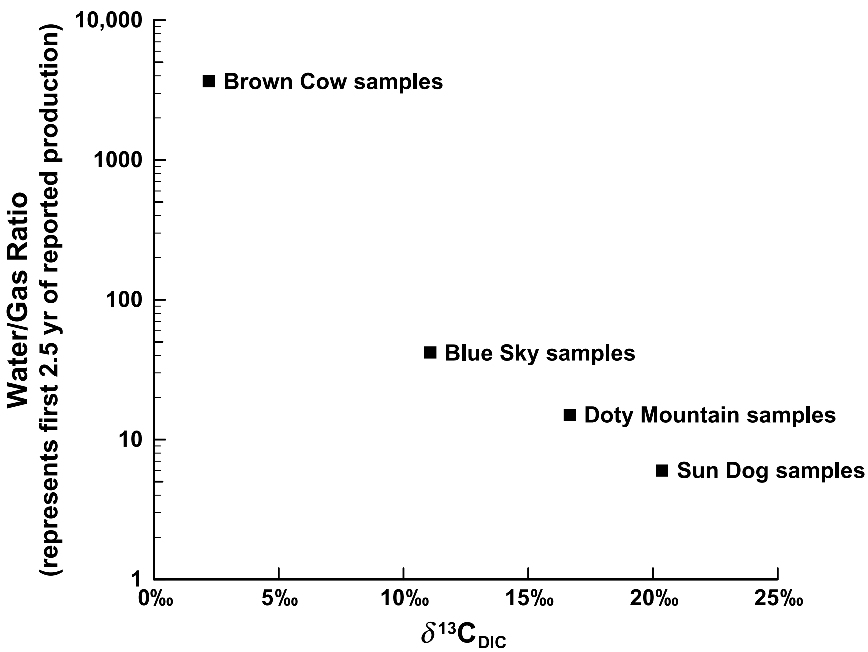

Figure 10. Average cumulative water/gas ratios for the first 30 months of reported production versus value for coalbed natural gas (CBNG) wells (WOGCC, 2010). Data from Table 3.

Atlantic Rim CBNG pods also record variations in cumulative water/gas ratios. These correlate strongly with $\delta^{13}C_{DIC}$, which is best illustrated by comparing Brown Cow and Sun Dog pods (Figure 10; Table 3). Both well sets were completed in 2004 and 2005 at similar depths and completions (Table 1). Brown Cow well samples have the lowest $\delta^{13}C_{DIC}$ values and the highest cumulative water/gas ratios (Figure 10; Table 3). Sun Dog well samples have the highest $\delta^{13}C_{DIC}$ and lowest cumulative water/gas ratios and are the most efficient and productive CBNG wells sampled in the Atlantic Rim.

Doty Mountain wells have the second highest $\delta^{13}C_{DIC}$ enrichment values and have the second lowest cumulative water/gas ratios (Figure 10; Table 3). Geochemical data indicate that most of Doty Mountain wells appear to be completed in confined reservoirs, and over time, the cumulative water/gas ratios of Doty Mountain wells have lowered (Table 3). Currently, Doty Mountain wells are second only to Sun Dog wells in the amount of gas they produce (WOGCC, 2010). Although Blue Sky wells produced more gas than Doty Mountain wells during the first 2.5 yr of production, they also produced more than three times the amount of water (Figures 9, 10; Table 3). As previously described, the low $\delta^{13}C_{DIC}$ values of interior Blue Sky wells suggest that these reservoirs are not as hydraulically confined as Doty Mountain reservoirs, and as a result, more water was produced to effectively desorb the gas.

A correlation between water/gas ratios, production potential, efficiency, and $\delta^{13}C_{DIC}$ is predicted: $\delta^{13}C_{DIC}$ should be less enriched in coalbed reservoirs that are hydraulically connected to multiple water sources with isotopically light carbon compositions. An unconfined coalbed reservoir is likely to produce more water during CBNG production than a confined coalbed reservoir, because the hydraulic pressure of multiple connected reservoirs would need to be reduced to promote CBNG desorption. Sun Dog wells, which have highly enriched $\delta^{13}C_{DIC}$ values and low cumulative water/gas ratios, appear to be producing from confined coalbed reservoirs (Figures 7A, 10; Table 3). Brown Cow wells, which are not as enriched regarding $\delta^{13}C_{DIC}$ and have high cumulative water/gas ratios, are likely producing from partially confined or unconfined coalbed reservoirs (Figures 7C, 10; Table 3).

Using $\delta^{13}C_{DIC}$ may help producers determine in which geographic areas coalbed reservoir water has undergone the most biologic methanogenic activity and/or those coalbed reservoirs that are confined. A contoured $\delta^{13}C_{DIC}$ map highlights the regional coalbed reservoirs with the greatest $\delta^{13}C_{DIC}$ enrichment (Figure 11). These highly enriched reservoirs are also the areas of peak CBNG production (Figure 11; Table 3) (WOGCC, 2010). Based on coalbed reservoir methanogenic enrichment trends, the northern segment of Dry Cow Creek has the highest potential for efficient CBNG production, and the southern areas of the Atlantic Rim show lesser potential for efficient CBNG production (Figure 11). Figure 11 also highlights the effects of faulting on enrichment trends, particularly in Blue Sky and Brown Cow wells. Note that all Brown Cow and Blue Sky wells have now been shut (WOGCC, 2010). We suggest that mapping $\delta^{13}C_{DIC}$ distributions would provide useful information for planning CBNG development.

Limitations of $\delta^{13}C_{DIC}$ in Coalbed Natural Gas Analysis

The enrichment of $\delta^{13}C_{DIC}$ is directly related to bacterial methanogenesis. The generation of thermogenic gas will not enrich DIC ratios, and $\delta^{13}C_{DIC}$ characterization is inapplicable in CBNG reservoirs that are exclusively thermogenic. Current models represent the Atlantic Rim as a mixed gas coalbed reservoir, where both thermogenic and biogenic gas are present, but only biogenic gas is fingerprinted by $\delta^{13}C_{DIC}$ of produced water. The $\delta^{13}C_{DIC}$ alone cannot identify which specific isotopically light reservoirs are in communication with coalbed reservoirs. Water quality, strontium isotopic compositions, well logs, and geologic interpretation of likely reservoirs may aid in distinguishing these reservoirs.

Recall that $\delta^{13}C_{DIC}$ analysis records the characteristics of the produced water at the time the wells were sampled. An important area of future

Figure 11. Regional $\delta^{13}C_{DIC}$ enrichment map of Atlantic Rim coalbed natural gas (CBNG) reservoirs. Note that $\delta^{13}C_{DIC}$ values are lower in the vicinity of faults.

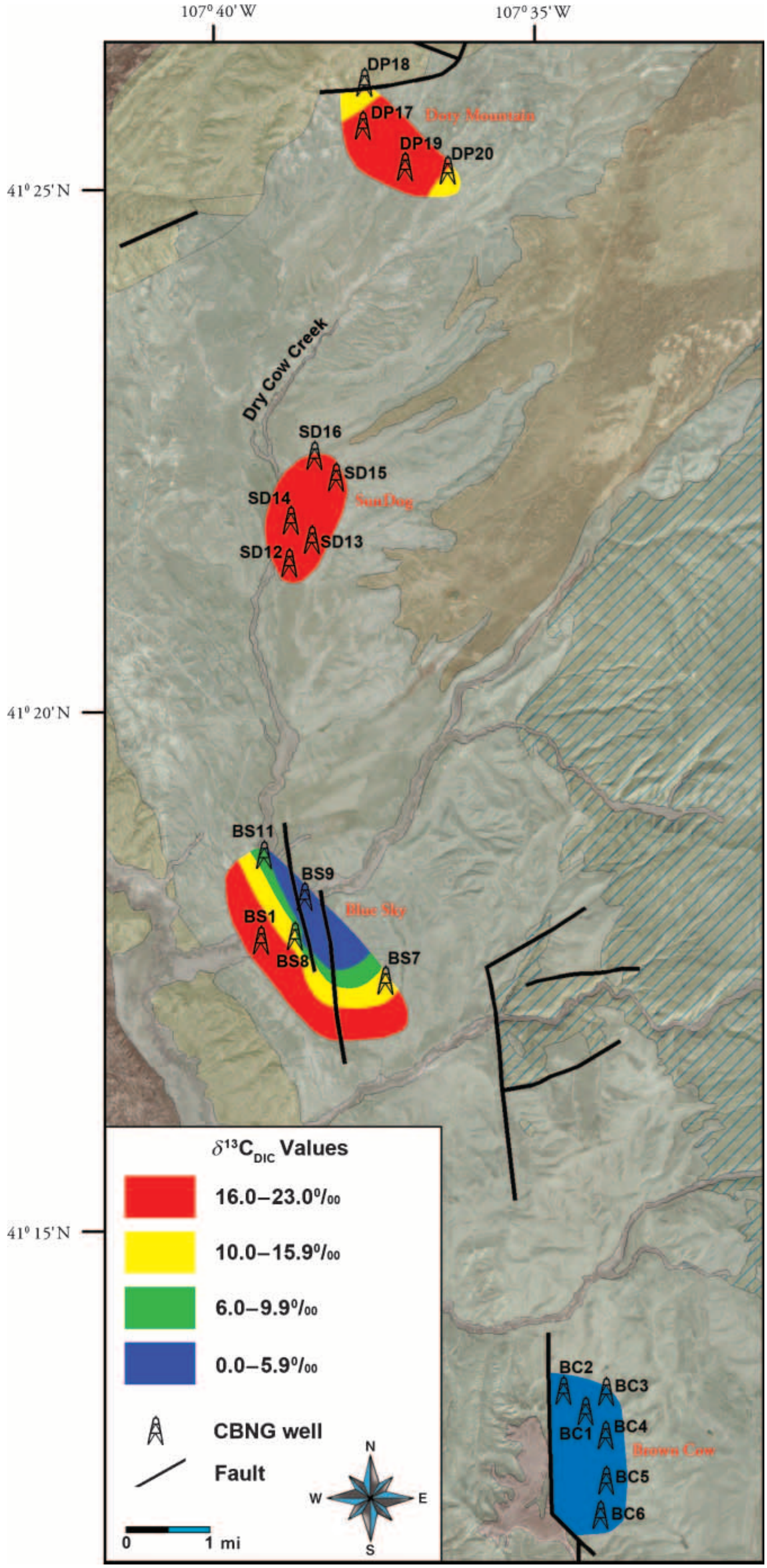

research is to document the evolution of $\delta^{13}C_{DIC}$ in individual wells over time so we can understand and relate any changes in water and gas production, as well as integrate the effects of operational procedures (i.e., completion and drilling techniques, pump efficiencies, etc.) on $\delta^{13}C_{DIC}$ values. For a better understanding of methane genesis, emplacement, and migration in Atlantic Rim coal beds, it would be useful to integrate isotopic data from gas analysis into future research, data which were unavailable for this study. In this study, we establish the value of using isotopic geochemistry of CBNG waters to characterize the nature and confinement of CBNG reservoirs; future research will explore additional aspects of gas production.

CONCLUSIONS

This study used major ion geochemistry, $^{87}Sr/^{86}Sr$, and $\delta^{13}C_{DIC}$ of surface water and groundwater to characterize the hydrology of the Atlantic Rim in Wyoming. The $\delta^{13}C_{DIC}$ in CBNG-produced water was used to identify Atlantic Rim CBNG reservoirs that have good hydrologic potential for efficient natural gas production.

Strontium isotopic composition and major ion geochemistry of surface water identified two distinct populations. Stream water and Mesaverde Group springs have Ca-Mg-SO_4–type water and higher $^{87}Sr/^{86}Sr$ values. Lewis Shale samples have sulfate reduced, Na-HCO_3–type water and low $^{87}Sr/^{86}Sr$ values.

An enriched $\delta^{13}C_{DIC}$ identifies groundwater in which biogenic production of methane has occurred. The $\delta^{13}C_{DIC}$ of groundwater that is not associated with methanogenesis has ratios of −7 to −15‰, whereas water coproduced with coalbed natural gas has ratios as high as +23‰. One group of Atlantic Rim springs have positive $\delta^{13}C_{DIC}$: enriched Lewis Shale springs have Na-HCO_3–type water, and some of them emit methane. Enriched Lewis Shale springs have higher TDS (800–4000 mg/L) than springs with negative $\delta^{13}C_{DIC}$ (TDS typically <1000 mg/L). These springs occur together in clusters updip of the CBNG production areas. The variations in abundance of methane emerging from these springs may be related to local variations in hydrostatic pressure of the near-surface methane-bearing reservoirs or influx from other gas-saturated coalbed reservoirs.

Although water produced with CBNG exhibit a wide range of $^{87}Sr/^{86}Sr$ values, all are Na-HCO_3–type water with relatively high TDS (>1000 mg/L) and positive $\delta^{13}C_{DIC}$. These data suggest that the water-rock interaction along subsurface flow paths resulted in different mean $^{87}Sr/^{86}Sr$, but that all CBNG water underwent sulfate reduction and methanogenesis. Water samples from wells with low water/gas ratios have the highest $\delta^{13}C_{DIC}$ and produce the most gas. Water samples from wells with lower, although still positive, $\delta^{13}C_{DIC}$ values reflect the addition of isotopically light water from other reservoirs. Structure contour mapping of the Mesaverde Group identifies faults in proximity to low $\delta^{13}C_{DIC}$ wells. The results of this study indicate that geochemical and isotopic analyses, particularly analysis of $\delta^{13}C_{DIC}$, help to identify Atlantic Rim CBNG reservoirs with the highest potential for natural gas production while minimizing unnecessary water production.

REFERENCES CITED

Aravena, R., S. M. Harrison, J. F. Barker, H. Abercrombie, and D. Rudolph, 2003, Origin of methane in the Elk Valley coal field, southeastern British Columbia, Canada: Chemical Geology, v. 195, p. 219–227, doi:10.1016/S0009-2541(02)00396-0.

Ayers Jr., W. B., and W. A. Kaiser, eds., 1994, Coalbed methane in the Upper Cretaceous Fruitland Formation, San Juan Basin, Colorado and New Mexico: University of Texas at Austin, Bureau of Economic Geology Report of Investigations, v. 218, 216 p.

Banner, J. L., M. L. Musgrove, and R. C. Capo, 1994, Tracing ground-water evolution in a limestone aquifer using Sr isotopes: Effects of multiple source of dissolved ions and mineral-solution reactions: Geology, v. 22 p. 687–690, doi:10.1130/0091-7613(1994)022<0687:TGWEIA>2.3.CO;2.

Bartos, T. T., L. L. Hallberg, J. P. Mason, J. R. Norris, and K. A. Miller, 2006, Water resources of Carbon County, Wyoming: U.S. Geological Survey Scientific Investigations Report 2006-5027, 191 p., http://pubs.usgs.gov/sir/2006/5027 (accessed September 20, 2010).

Botz, R., H. D. Pokojski, M. Schmitt, and M. Thomm, 1996, Carbon isotope fractionation during bacterial methanogenesis by CO_2 reduction: Organic Geochemistry, v. 25, p. 255–262, doi:10.1016/S0146-6380(96)00129-5.

Brinck, E. L., J. I. Drever, and C. D. Frost, 2008, The geochemical evolution of water co-produced with coal bed natural gas in the Powder River Basin, Wyoming: Environmental Geosciences, v. 15, no. 4, p. 153–171, doi:10 .1306/eg.01290807017.

BLM (Bureau of Land Management), 2007, Final environmental impact statement (FEIS) for the Atlantic Rim natural gas field development project Carbon County, Wyoming, November 2006: Rawlins Bureau of Land Management, Department of the Interior: FR Doc. E6-12952; http://www.blm.gov/wy/st/en/info/NEPA/rfodocs/atlantic_rim.html (accessed September 20, 2010).

Clark, I., and P. Fritz, 1997, Environmental isotopes in hydrogeology: Boca Raton, Florida, Lewis Publishers, 328 p.

Clarke, R. W., 1916, The data of geochemistry 3d edition: U.S. Geological Survey Bulletin, v. 616, 821 p.

Collerson, K. D., W. J. Ullman, and T. Torgersen, 1988, Ground-waters with unradiogenic $^{87}Sr/^{86}Sr$ ratios in the Great Artesian Basin, Australia: Geology, v. 16, p. 59–63, doi:10.1130/0091-7613(1988)016<0059:GWWUSS>2.3.CO;2.

Frost, C. D., and R. N. Toner, 2004, Strontium isotopic identification of water rock interaction and groundwater mixing: Ground Water, v. 42, no. 3, p. 541–568.

Hellings, L., K. van den Driessche, W. Baeyens, E. Keppens, and F. DeHairs, 2000, Origin and fate of dissolved inorganic carbon in interstitial waters of two freshwater intertidal areas: A case study of the Scheldt Estuary, Belguim: Biogeochemistry, v. 51, p. 141–160, doi:10 .1023/A:1006472213070.

Hettinger, R. D., and L. N. R. Roberts, 2005, Lewis total petroleum system of the southwestern Wyoming province, Wyoming, Colorado, and Utah: Petroleum Systems and Geologic Assessment of Oil and Gas in the Southwestern Wyoming Province, Wyoming, Colorado, and Utah, Chapter 9: U.S. Geological Survey Southwestern Wyoming Province Assessment Team: U.S. Geological Survey Digital Data Series DDS-69-D, 2005, 39 p.

Hettinger, R. D., J. G. Honey, M. S. Ellis, C. S. V. Barclay, and J. A. East, 2008, Geologic map of Upper Cretaceous and Tertiary strata and coal stratigraphy of the Paleocene Fort Union Formation, Rawlins-Little Snake River Area, south-central Wyoming: U.S. Geological Survey Scientific Investigations Map 3053, 3 sheets.

Johnson, R. C., T. M. Finn, and L. N. R. Roberts, 2005, The Mesaverde total petroleum system, southwestern Wyoming province petroleum systems and geologic assessment of oil and gas in the southwestern Wyoming province, Wyoming, Colorado, and Utah, Chapter 8: U.S. Geological Survey Southwestern Wyoming Province Assessment Team: U.S. Geological Survey Digital Data Series DDS-69-D, 39 p.

Lamarre, R. A., and S. K. Ruhl, 2004, Atlantic Rim coalbed methane play: The newest successful CBM play in the Rockies (abs.): Rocky Mountain Section of the AAPG 2004 Annual Meeting, 1 p., http://www.searchanddiscovery.net/documents/abstracts/2004rocky/index.htm (accessed September 2010).

Love, J. D., and A. C. Christiansen, 1985, Geologic map of Wyoming: U.S. Geological Survey, scale 1:500,000, 3 plates.

Martini, A. M., L. M. Walter, J. M. Budai, T. C. W. Ku, C. J. Kaiser, and M. Schoell, 1998, Genetic and temporal relations between formation waters and biogenic methane; Upper Devonian Antrim Shale, Michigan Basin, U.S.A.: Geochimica et Cosmochimica Acta, v. 62, no. 10, p. 1699–1720, doi:10.1016/S0016-7037(98)00090-8.

McIntosh, J. C., A. M. Martini, S. Petsch, and K. Nüsslein, 2008, Biogeochemistry of the Forest City Basin coalbed methane play: International Journal of Coal Geology, v. 76, p. 111–118, doi:10.1016/j.coal.2008.03.004.

McLaughlin, J. F., 2009, Stable and radiogenic isotopic analysis of aquifer systems, Atlantic Rim, Carbon County, Wyoming: Implications for production of coal bed natural gas: M.S. thesis, University of Wyoming, Laramie, Wyoming, 76 p., 1 plate.

Mook, W. G., and F. C. Tan, 1991, Stable carbon isotopes in rivers and estuaries, *in* E. Degens, S. Kempe, and J. Richey, eds., Biogeochemistry of major world rivers: New York, John Wiley and Sons, p. 245–264.

Pashin, J. C., 2007, Hydrodynamics of coalbed methane reservoirs in the Black Warrior Basin: Key to understanding reservoir performance and environmental issues: Applied Geochemistry, v. 22, p. 2257–2272, doi:10.1016/j .apgeochem.2007.04.009.

Pashin, J. C., W. E. Ward II, R. B. Winston, R. V. Chandler, D. E. Bolin, K. E. Richter, W. E. Osborne, and J. C. Sarnecki, 1991, Regional analysis of the Black Creek–Cobb coalbed-methane target interval, Black Warrior Basin, Alabama: Alabama Geological Survey Bulletin, v. 145, 127 p.

Pitman, J. K., J. C. Pashin, J. R. Hatch, and M. B. Goldhaber, 2003, Origin of minerals in joint and cleat systems of the Pottsville Formation, Black Warrior Basin, Alabama: Implications for coalbed methane generation and production: AAPG Bulletin, v. 87, p. 713–731, doi:10.1306/01140301055.

Roehler, H. W., 1990, Stratigraphy of the Mesaverde Group in the central and eastern Greater Green River Basin, Wyoming, Colorado, and Utah: U.S. Geological Survey Professional Paper 1508, 52 p.

Roehler, H. W., 1992, Introduction to Greater Green River Basin geology, physiography, and history of investigations: U.S. Geological Survey Professional Paper 1506-A, 14 p, 1 plate.

Scott, A. R., W. R. Kaiser, and W. B. Ayers Jr., 1994, Thermogenic and secondary biogenic gases, San Juan Basin, Colorado and New Mexico: Implications for coalbed gas producibility: AAPG Bulletin, v. 78, p. 1186–1209.

Sharma, S., and C. D. Frost, 2008, An innovative approach for tracing coalbed natural gas coproduced water using stable isotopes of carbon and hydrogen: Groundwater, v. 46, no. 2, p. 329–334.

Simpkins, W. W., and T. B. Parkin, 1993, Hydrogeology and redox geochemistry of CH_4 in a late Wisconsinian till and loess sequence in central Iowa: Water Resources Research, v. 29, p. 3643–3657, doi:10.1029/93WR01687.

Souders, A. K., and C. D. Frost, 2006, In suspect terrane? Provenance of the late Archean Phantom Lake metamorphic suite, Sierra Madre, Wyoming: Canadian Journal of Earth Sciences, v. 43, no. 10, p. 1557–1577, doi:10.1139/E06-114.

Steidtmann, J. R., 1993, The Cretaceous foreland basin and its sedimentary record, *in* A. W. Snoke, J. R. Steidtmann, and S. M. Roberts, eds., Geology of Wyoming: Geological Survey of Wyoming Memoir 5, p. 250–271.

Surdam, R. C., Z. Jiao, K. E. Clarey, R. H. DeBruin, R. D. Bentley, J. E. Stafford, A. Deiss, and M. Ewald, 2007, An evaluation of coalbed methane production trends in Wyoming's Powder River Basin: A tool for resource management: Wyoming State Geological Survey, CGRD-3, 43 p.

Van Voast, W. A., 2003, Geochemical signature of formation waters associated with coalbed methane: AAPG Bulletin, v. 87, no. 4, p. 667–676, doi:10.1306/10300201079.

Whiticar, M. J., 1999, Carbon and hydrogen isotope systematics of bacterial formation and oxidation of methane: Chemical Geology, v. 161, p. 291–314, doi:10.1016/S0009-2541(99)00092-3.

WOGCC (Wyoming Oil and Gas Conservation Commission), at http://wogcc.state.wy.us/ (accessed 2007–2009).